Stimulated release of intraluminal vesicles from Weibel-Palade Bodies

James Streetley[1† ‡], Ana-Violeta Fonseca[1‡], Jack Turner[2] Nikolai I. Kiskin[1¶], Laura Knipe[1#], Peter B. Rosenthal[1,2], Tom Carter[1,3]

[1]MRC National Institute for Medical Research, The Ridgeway, London NW7 1AA [2]Structural Biology of Cells and Viruses Laboratory, The Francis Crick Institute, 1 Midland Road, London NW1 1AT. [3]Molecular and Clinical Sciences Research Institute, St George's University, London, SW17 0RE.

Present addresses: [†]J.S., MRC-University of Glasgow Centre for Virus Research, Sir Michael Stoker Building, 464 Bearsden Road, Glasgow, G61 1QH. [¶]N.I.K., Flat 15 Holmdene, Holden Road, London N12 8HU. [#]L.K.,The Francis Crick Institute, 1 Midland Road, London NW1 1AT.

[‡]These authors contributed equally.

Running head: Intra-luminal vesicles of WPBs

Corresponding Authors: Prof. Tom. Carter,
Molecular and Clinical Sciences Research Institute,
St George's University,
London,
SW17 0RE
tcarter@sgul.ac.uk

Dr. Peter B. Rosenthal,
Structural Biology of Cells and Viruses Laboratory
The Francis Crick Institute
1 Midland Road,
London NW1 1AT
Peter.Rosenthal@crick.ac.uk

Category: Regular article

Abstract:	159
Main text:	3962
Figures:	7
Refs:	64

Key Points:

- Weibel-Palade bodies (WPBs) contain CD63-positive intraluminal vesicles that are released during secretagogue-evoked exocytosis.
- Cryo-electron microscopy of intact vitrified endothelial cells reveal intraluminal vesicles as a novel structural feature of WPBs.

Abstract

Weibel-Palade bodies (WPBs) are secretory granules that contain von Willebrand factor and P-selectin, molecules that regulate hemostasis and inflammation respectively. The presence of CD63/LAMP3 in the limiting membrane of WPBs has led to their classification as lysosome-related organelles. Many lysosome-related organelles contain intraluminal vesicles (ILVs) enriched in CD63 that are secreted into the extracellular environment during cell activation to mediate intercellular communication. To date there are no reports that WPBs contain or release ILVs. By light microscopy and live-cell imaging we show that CD63 is enriched in micro-domains within WPBs. Extracellular antibody recycling studies showed that CD63 in WPB micro-domains can originate from the plasma membrane. By cryo-electron tomography of frozen-hydrated endothelial cells we identify internal vesicles as a novel structural feature of the WPB lumen. By live-cell fluorescence microscopy we observe directly the exocytotic release of EGFP-CD63 ILVs as discrete particles from individual WPBs. WPB exocytosis provides a novel route for release of ILVs during endothelial cell stimulation.

Key Words: electron cryomicroscopy, endothelial cells, Weibel-Palade body, intra-luminal vesicle, von Willebrand factor, exosome, CD63, P-selectin.

Introduction

Endothelial cells regulate hemostasis and inflammation through direct cell-cell contacts, secretion of soluble or membrane associated mediators, and through the release of small bioactive lipid vesicles (extracellular vesicles; EVs). Many of the soluble secreted molecules, such as the adhesive glycoprotein von Willebrand Factor, are stored and released in a regulated fashion from specialized secretory granules called Weibel-Palade bodies (WPBs) [1]. EVs can arise by several distinct mechanisms: (1) exocytosis of late endosomes/multivesicular bodies (LE/MVBs) to release intra-luminal vesicles (ILVs; termed exosomes upon secretion) (2) budding from the plasma membrane (shedding micro-vesicles or ecotosomes), or (3) plasma membrane blebbing during programmed cell death (apoptotic bodies). EVs contain a variety of signaling molecules that modulate gene expression and function of target cells, and are now widely viewed as important mediators of intercellular communication and control [2].

WPBs form at the trans-Golgi network (TGN) through a pH- and Ca^{2+}-dependent condensation of von Willebrand factor (VWF) and the VWF-propolypeptide (VWFpp) to form helical tubule structures [3-5]. VWF-VWFpp tubules comprise the majority of the protein content of WPBs and give the organelle its distinctive morphology [3]. The leukocyte adhesion molecule P-selectin is also stored in the WPB limiting membrane and upon release into the plasma membrane it mediates the tethering and rolling of leukocytes on the vessel wall prior to extravasation at sites of inflammation. Efficient P-selectin-mediated leukocyte capture requires the tetraspanin CD63 (also called LAMP3) that is also present in the limiting membrane of WPBs and co-released to the plasma membrane during exocytosis [6-8]. P-selectin enters WPBs during their formation at the TGN, however, CD63 is delivered to WPBs at a later stage through a poorly defined interaction with LE\MVBs [9,10] requiring the endosomal sorting complex AP-3 and annexin 8 [7,10].

The interaction of WPBs with endosomal components, their acidic lumenal pH, and acquisition of CD63/LAMP3 have led to the WPBs classification as a lysosomal-related organelle (LRO) [11], a

functionally diverse set of compartments containing different cargoes that none-the-less share certain features or components with lysosomes. LRO biogenesis is complex and organelle-specific: Some form by re-modeling/maturation of endosomal compartments (e.g. MVBs, secretory lysosomes, melanosomes), some originate from the TGN (WPBs), while others may involve contributions from both pathways (e.g. lytic granules, platelet granules) [11].

LROs that undergo fusion with the plasma membrane to release their contents include the major histo-compatibility complex class II-enriched compartment of B lymphocytes, lytic granules of cytotoxic T cells, platelet dense core and α-granules, basophilic granules, lamellar bodies of lung epithelia cells, osteoclast granules, sperm acrosomes and WPBs [12,13]. In most cases the delivery of these organelles to the plasma membrane, and their exocytosis, is regulated by "secretory Rab proteins" and their effector molecules. For WPBs, these include Rab27A, MyRIP, Slp4-a and Munc13-4 [14-17]. Some LRO's contain ILVs that can be released during fusion with the plasma membrane [12,18,19], and unsurprisingly several key regulators of WPB and other LRO exocytosis (e.g. Rab27A, Slp4-a) also control exosome release [20,21]. Despite their classification as LROs and sharing a common set of molecular components regulating exocytosis, it is not known whether WPBs contain or release ILVs. Using live-cell imaging and high-resolution cryo-EM tomography of vitrified endothelial cells we identify and characterize ILVs in WPBs. We directly demonstrate the exocytotic release of EGFP-CD63 enriched ILVs from individual WPBs during hormone-stimulation. This is a new route for EV release from endothelial cells and extends the range of signaling modalities through WPBs.

Methods

Endothelial cell culture, transfections, immunocytochemistry, antibodies, DNA constructs and reagents

Human umbilical vein endothelial cells (HUVEC) or human heart microvasculature endothelial cells (HHMEC) were purchased, cultured, Nucleofected and processed for immunocytochemistry as previously described [15,22]. VWF-mRFP or -mCherry, VWFpp-mRFP, VWFpp-mEGFP, mRFP-Rab27A and EGFP-CD63 have been described previously (see [15] and references therein). Rabbit anti-VWF (A0082, 1:10000 dilution) was from Dako Ltd (Ely, UK), rabbit anti-VWFpp (1:500) is described in [23], mouse anti-LBPA (Z-PLBPA, 1:1000) was from Tebu-bio (Peterborough, UK), mouse anti-P-selectin (clone AK6, 1:50) was from Serotec (Kidlington, UK), rabbit anti-VPS2B (ab33174, 1:300) and mouse anti-Alix (ab117600, 1;300) were from Abcam (Cambridge, UK), rabbit anti-syntenin (133003, 1:100) was from Synaptic Systems GmbH (Gottingen, DE), mouse anti-TSG101 (GTX70255) and rat anti-HSP70 (GTX191366) were from GeneTex (Irvine, CA), mouse anti-CD9 (clone HI9a, 1:1000), anti-CD81 (clone 5A6, 1;1000) were from Biolegend (London, UK), mouse anti-CD63 (clone H5C6, 1;200) was from the Developmental Studies Hybridoma Bank (see Acknowledgments), normal mouse IgG_1 (SC-3877, 1;55) and mouse anti-CD63-TRITC (SC-5275, 1:55) were from Insight Biotechnology ltd (Wembly, UK), from Abcam. Secondary antibodies coupled to fluorophores (1:200) were from Jackson Immunoresearch (USA). All other reagents were from Sigma-Aldrich unless otherwise stated.

Cell culture on electron microscopy grids, electron cryomicroscopy and image and tilt series and tomogram analysis.

HUVEC or HHMEC were grown on carbon film on gold grid supports for microscopy as previously described [3]. Gold grids with cells on were washed briefly in PBS and 4 µl of 40% protein A conjugated 10nm gold colloid (BBI Life Sciences) in PBS added between washing and freezing, to act as fiducial markers. WPBs were imaged in cells either unstimulated or following

stimulation. For stimulation PBS contained 100 µM histamine dihydrochloride or ionomycin (300nM or 1 µM ionomycin, Streptomyces conglobatus).

Grids were frozen by plunging into liquid ethane using either a manual plunge-freezer or an FEI Vitrobot Mark III (FEI Company) at either at room temperature and humidity (manual) or at 22°C and room humidity (Vitribot; humidifier switched to off). Frozen grids were stored in liquid N_2. Frozen grids were imaged using either a Spirit TWIN microscope (FEI) operating at 120 kV and equipped with an Eagle 2k camera (FEI) using a Gatan 626 cryotomography holder or a LN_2 cooled Polara microscope (FEI) operating at 200 kV and equipped with a F224 CCD camera (TVIPS). Both TIA (FEI) and SerialEM [63] image acquisition software were used, and low-dose procedures were used in both packages. SerialEM was used to collect whole grid montages at ~140x magnification, which were used for locating areas of interest for further imaging using low-dose procedures.

Single-axis tilt-series were collected automatically using SerialEM, with an angular range of -60° to +60° and increment of 2° or 3°. Total dose for tilt-series were limited to 50 to 70 e^-/A^2, giving individual images with a dose of 1.2 to 1.7 e^-/A^2. The dose per image was kept constant for each tilt angle in a series. The target defocus was set at -8 µm. Tomographic tilt series were aligned using fiducials using Etomo from the in IMOD software [24]. Projection images in aligned tilt series were normalized based on their histograms and reconstructed to 3D volumes and analyzed as previously described [3].

Image and volume analysis.

Simple image processing tasks such as crop, pad and rotate were performed in Ximdisp and FFT calculations were performed using Ximdisp and _trans from the MRC suite. Figures were prepared using Photoshop CS4 (Adobe). Amira (FEI Visualization Sciences Group), and IMOD were used to generate 3D models.

VWF tubules were manually traced using IMOD. Tomograms were segmented using the Amira 'Segmentation' tool. Membranes and tubules were rendered and displayed in Amira.

Live cell fluorescence imaging, confocal FRAP and analysis.

Nucleofected cells were plated at confluent density in culture medium onto 35 mm diameter poly d-lysine coated glass glass-bottomed culture dishes (MatTeK corp. Ashland, USA) or 25 mm diameter glass coverslips (#1.0, 0.15 mm, VWR International, UK). 25 mm diameter glass coverslips were mounted in Rose chambers containing physiological saline (in mM): NaCl- 140, KCl- 5, $MgSO_4$- 1, $CaCl_2$- 2, Glucose- 10, HEPES- 20, pH 7.3 (adjusted with NaOH). High speed dual-color epifluorescence imaging was carried out on an Olympus IX71 inverted microscope equipped with an Olympus UPLSAPO x100 oil 1.40NA objective, a 1.6x magnifier and an Ixon3 EMCCD camera operated in frame transfer mode at full gain and cooled to –70ºC (Andor, Belfast, United Kingdom). Full frame images were acquired at 30 frames s^{-1}. High-speed single or sequential dual color excitation wavelength switching (470±40nm and 572±35nm) was by OptoLED (Cairn Research, Faversham, UK), the excitation filter set comprising a GFP/DsRed dual band dichrochic mirror (Chroma part 51019) and a GFP/DsRed dual band emitter. Image capture and wavelength switching was synchronized using WinFluor software (Dr John Dempster, Strathclyde University, Glasgow, United Kingdom). The microscope was housed within an environmental chamber maintained at 36ºC and cells stimulated with histamine (100µM). Confocal FRAP experiments were carried out using Leica Microsystems TCS SP2 or SP5 (8 kHz resonant scanner) confocal microscopes equipped with Leica HCX PL APO x63 1.32NA (SP2) or HCX PLAPO CS x100 oil-immersion objectives with NA of 1.40 (SP2) or 1.46 (SP5) as previously described [15,25,26]. Excitation (bidirectional "fly" FRAP mode) was at 488nm (EGFP) and 561nm (mRFP). Emission windows for single-wavelength (EGFP) were 495-620nm and for dual-colour (EGFP, mRFP; simultaneous "fly" mode excitation) were, EGFP;500-545 nm, mRFP;585-750nm. Images from SP2 were collected at 512x128 (or 64) pixels and at zooms 20-32, and from SP5 at 512x300 pixels at zooms between 19.1 and 38.8. FRAP imaging

and ROIs were set as previously described [15,25,26] and single or dual-color bleaching applied during 2-10 consecutive frames acquired at 0.344 seconds (SP2) and between 0.792 and 0.962 was seconds (SP5). Images were background-subtracted and analyzed using custom-made macros implemented in ImageJ (http://rsb.info.nih.gov/ij/) [26]. Image montages and AVI video clips (Jpeg compression) were made in ImageJ2\Fiji. Data plots were made in Origin 9.2 (OriginLab Corporation, Northampton, USA). Results are expressed as mean ± s.e.m.

Results

Enrichment of CD63 in discrete micro-domains within WPBs

Tetraspanins, including the ubiquitously expressed CD63, are amongst the most common endosomal components enriched in secreted ILVs [27,28] (http://www.exocarta.org/), and CD63 in particular is implicated in cargo sorting to exosomes [29]. Consequently CD63 is widely used as a marker to identify, visualize and track ILVs/exosomes within and between cells [30]. To determine if WPBs contained CD63-enriched regions we first analyzed the pattern of endogenous CD63 in WPBs by immunocytochemistry (Figure 1A). Consistent with previous studies CD63-immunoreactivity was seen on both WPBs and other endomembrane compartments [31]. Close inspection revealed discrete bright "micro-domains" of CD63-immunoreactivity associated with some WPBs, often near the ends of the organelle but also at intermediate points up to mid-body (Supplementary Figure S1A). Expression of EGFP-CD63 produced similar features (Figure 1B), and crucially, live-cell fluorescence imaging showed that the EGFP-CD63 micro-domains were connected to and moved with (but not within) the WPB (See Supplementary videos S1 and S2). Measurement of WPB EGFP-CD63 fluorescence intensity in live cells showed the micro-domains to be stable in intensity and up to 4-5 times brighter than the bulk signal in the WPB membrane (Figure 1C), reminiscent of the enrichment reported for CD63 in ILVs of LE/MVBs and exosomes [32]. Further immunofluorescence analysis showed that other WPB membrane proteins (Rab27A, P-selectin) were present in the limiting membrane of the granule but were not concentrated in CD63-rich micro-domains (Supplementary Figure S1B).

At the plasma membrane, tetraspanins can form enriched areas or microdomains that appear as long-lived "spot-like" structures in which contributing tetraspanins, and associated proteins, are in dynamic exchange with the bulk plasma membrane on a time scale of seconds [33]. To examine if EGFP-CD63 in the WPB limiting membrane was in diffusional equilibrium with CD63 microdomains we used single WPB FRAP analysis in EGFP-CD63 and VWF-mRFP co-expressing HUVEC [25,26] Consistent with our previous studies[25] EGFP-CD63 was freely mobile in the WPB limiting membrane,

undergoing rapid and complete recovery, by lateral membrane diffusion, after each period of bleaching (Supplementary Figure S2, and Supplementary video S3). The core protein VWF-mRFP was used to confirm the organelle's identity, and was completely immobile showing no recovery after bleaching, as previously reported [25]. Our FRAP analysis showed that EGFP-CD63 in micro domains did not contribute to recovery of EGFP-CD63 fluorescence within the limiting membrane nor did micro domains re-accumulate fluorescence from the WPB limiting membrane when selectively bleached (Supplementary Figure S2). The results indicate that EGFP-CD63 in microdomains is not in diffusional equilibrium with EGFP-CD63 in the WPB limiting membrane.

Intra-luminal vesicles in WPBs revealed by cryo-electron tomography

The presence of micro-domains containing the membrane tetraspanin CD63 but topologically separated from the WPB membrane suggested that these were ILVs. To test this we applied high-resolution electron cryomicroscopy to image the thin edge of plunge-frozen, whole mount HUVECs, an approach that we have previously shown to reveal the high-resolution architecture of organelles without chemical fixation or staining [3]. In 2D projection images, WPBs appear as rod-shaped granules denser than the surrounding cytoplasm (Figure 2A-C) containing tubules of VWF which are the source of the signature helical pattern in their Fourier transforms (Figure 2B, inset). We can identify ILVs in these images (arrows). In fact, 12% of 535 2D images show evidence for at least one and up to three ILV's per granule. To clearly identify the internal vesicles in the context of granule architecture without the ambiguity of overlap in the 2D image, we performed electron cryotomography and volume reconstruction. Figure 3 (and Supplementary video S4) shows a tomogram section containing WPBs, other vesicular organelles, cytoskeletal filaments, ribosomes, and other particles. ILVs within WPBs are indicated by arrows. The lumen of WPB ILVs was less electron dense than the surrounding VWF tubules, being similar in density to the lumen of ILVs of MVBs and to regions of cell cytosol.

We built structural models for 22 ILVs from 15 tomograms (Figures 4, 5 and Supplementary Figure S3). ILVs were not confined to regions close to the ends of WPBs, but could be seen at any point up to mid-body. In many cases the membrane of the ILV was in close apposition to the WPB limiting membrane and sometimes associated with a bulge in the WPB limiting membrane. ILVs were often non-spherical in shape, appearing compressed between the smooth limiting membrane of the WPB and VWF tubules. As previously observed WPBs contained paracrystals of helical VWF, shown in cross section as indicated in Figure 4A and Supplementary video S5. A prominent membrane-bounded ILV can be seen where the paracrystalline packing is disrupted giving the granule a club-shape, a common morphology for WPBs. WPB ILVs were also observed in adult human heart microvascular endothelial cells (HHMEC) (Figure 4B and Supplementary Figure S3C) confirming that these structures are not specific to HUVEC but represent a general feature of endothelial WPBs.

We observed many WPB ILVs of HUVEC or HHMEC to contain densities and structures resembling cytoplasmic components (Figure 4 B,C and Supplementary Figure S4 and video S6). Measurements of WPB ILVs and ILVs of single- and multi-vesicular bodies (MVBs) and single internal vesicle bodies in tomograms (Figure 5) showed them to have a similar size distribution and include some large outliers (e.g. ILV in WPB in Supplementary Figure S3A). The majority of ILVs in WPBs (mean volume 147,292±41,225 nm^3, sem, n=15 measurements) are similar in size to the small vesicles within the MVBs (mean volume 165,286±30,664 nm^3, sem, n=25) (see Supplementary video S7).

WPB ILVs contain CD63 derived from the endocytic pathway but may differ in composition from ILVs in MVBs

Because endogenous CD63 cycles from the plasma membrane to WPBs via the endocytic pathway [7,9,10] we next examined whether CD63 in WPB ILVs was also derived from this trafficking route by monitoring the accumulation of an extracellularly applied TRITC-labelled mouse anti-human CD63 antibody in WPBs as previously described [7] (Figure 6). The TRITC-anti-CD63 antibody (but not a

non-targeting mouse IgG_1 control antibody, Supplementary Figure S5) was readily trafficked to WPBs (Figure 6A) and in both control and EGFP-CD63-expressing HUVEC was enriched within WPB ILVs (Figure 6B-C) confirming that WPB ILV CD63 is of endosomal origin. We next looked for evidence in WPB-ILVs of other components reported to be present in ILVs of endosomal origin. Biochemical studies have identified cholesterol as one of the lipids enriched in exosomes [34]. Localization of cholesterol-rich regions by filipin staining in HUVEC, showed abundant labelling of endosomal/lysosomal structures but no labelling of WPBs (Supplementary Figure S6C). Some [35] but not all [36] studies suggest that LE/MVBs and their ILVs are enriched in lysobisphosphatidic acid (LBPA). Immuno-staining of HUVEC for endogenous LBPA, showed a striking punctate enrichment within LE/MVBs but no labelling of WPBs (Supplementary Figure S6Ai), a result consistent with a previous study [9]. The fluorescent phosphatidyl ethanolamine (PE) analogue, N-Rh-PE (1,2-dipalmitoyl-sn-glycero-3-phosphoethanolamine-N-[lissamine rhodamine B sulfonyl]), is taken up from the plasma membrane, trafficked to LE\MVBs and incorporated into exosomes [37,38]. Incubation of HUVEC with N-Rh-PE revealed no WPB staining (Supplementary Figure S6Bi-ii). Other common exosomal markers, including CD9, CD81, along with several ESCRT components including Alix, TSG101, VSP2/Chmp2B, HSP70 and the autophagy marker LC3 were not detected in WPBs (Supplementary Figures S7 and S8). However, we did detect the PDZ domain containing adapter protein, syntenin, associated with WPBs (Supplementary Figure S8B). Together the results suggest WPB ILVs have a distinct composition.

Direct observation of ILV secretion during WPB exocytosis

Having established that WPBs do contain ILVs we next asked whether these could be released during exocytosis. If so, we predicted that WPB associated EGFP-CD63 microdomains (ILVs) would be released as discrete fluorescent particles during WPB exocytosis. To test this we monitored histamine-evoked WPB exocytosis in live HUVEC co-expressing VWF-mCherry and EGFP-CD63 using high-speed epifluorescence imaging. EGFP-CD63 labeled ILVs were released as discrete

particles from individual WPBs during histamine stimulation (Figure 7). Panels A-D show image sequences taken from Supplementary videos S8, S9, S10 and S11 respectively. In examples A-C the EGFP-CD63 particles (arrows) escape rapidly into the bulk solution and are lost from view. D shows an example of the particle becoming trapped within the extracellular patch of VWF secreted during WPB exocytosis. In addition to direct release into the bulk solution the particles were also secreted into the narrow two-dimensional plane between the cell and the glass coverslip. In these cases the extracellular diffusion of the particles could be visualized for long periods before the particles eventually encountered the cell edge and escaped into the bulk media (e.g. Supplementary video S12). Consistent with our ultrastructural data, we also observed release of multiple ILVs from single WPB (Supplementary video S13). Thus CD63-containing ILVs are released from the interior of the WPB to the extracellular medium along with VWF during exocytosis.

Discussion

Here we demonstrate that WPBs contain CD63-postive ILVs and release them during secretagogue-evoked exocytosis. Shedding of plasma membrane-derived vesicles and MVB-plasma membrane fusion has been visualized in live cells [21,39,40], however, direct imaging of ILV release from individual regulated secretory granules during exocytosis has not been reported previously. To indicate their specific origin, we refer to the secreted vesicles described here as WPB-released exosomes.

Our cryomicroscopy studies of the thin periphery of endothelial cells show that mature WPBs contain ILV's that are either embedded within and distort the paracrystalline assemblies of VWF tubules or are squeezed between the VWF paracrystal and the tightly wrapped granule-limiting membrane. This accounts for their immobility within the granule.

During exocytosis WPB-released exosomes are secreted into the surrounding medium, although they may initially be entangled by the secreted VWF. In other systems, tethering has been proposed as a mechanism of restricting exosomes to local target sites [41]. WPB exocytic events involve complex structural changes in the granule [1] and may selectively release small molecules to the bloodstream as well as CD63 to the plasma membrane without releasing VWF [42]. ILV release adds an additional signaling diversity to these exocytic events.

The identification of CD63-rich ILV's within the WPB lumen extends the features that WPBs share with other LROs. Many LROs, such as melanosomes and lytic granules, release CD63-rich vesicles. Our observations draw further attention to the similarity of WPBs to platelet α-granules which originate as MVBs containing ILVs, but during maturation become filled with dense material, including VWF and P-selectin. In addition, our immunofluorescence data show that WPB ILVs are enriched in CD63 but lack CD9 or CD81, which is also the case with the ILVs of platelet α-granules [18].

In contrast to platelet α-granules, WPBs form by the polymerization of VWF in nascent granules at the TGN. Protrusive clathrin-coated membrane buds are a feature of nascent WPBs, reflecting the active sorting away of material not destined for storage in the mature WPB [43]. Mature WPBs lack bilayer coats [3,43,44] and our cryo-EM images of vitrified endothelial cells show a tight, almost shrink wrapped limiting membrane surrounding the paracrystalline core of VWF and associated ILVs.

Newly forming WPBs emerging from the TGN lack CD63, but soon after acquire the tertraspannin through a poorly defined interaction with endosomal components [9,10] that involve the adapter protein AP3 and Annexin 8 [7,10]. These observations (on WPBs and platelet α-granules) contribute to a view in which the LRO possesses a mixture of endosomal vs regulated secretory features that depend on the organelle's biogenesis and specialisation.

In this study we have shown that the CD63 in WPB ILVs is trafficked via the endosomal system. CD63 is a ubiquitously expressed integral membrane protein found on the plasma membrane and endosomal compartments of all cells [45]. In endosomal compartments CD63 is enriched in a subset of ILVs and is present on exosomes secreted during MVB fusion with the plasma membrane [34,46,47]. CD63 delivery to WPBs could occur through small vesicles formed by endosomal membrane budding [48]. Such vesicles can contain AP3 [49], the adapter protein implicated in CD63 delivery to WPBs [10]. Alternatively, direct fusion and content transfer between LE\MVBs and lysosomal compartments is well documented [50] and a similar process could account for diffusional transfer of CD63 to the limiting membrane of the maturing WPB, as well as direct MVB to WPB ILV transfer. The absence in WPBs of several markers reported to be enriched in ILVs/exosomes of LE/MVBs; Lysobisphosphatidic acid (LPBA) [9], cholesterol [36], CD9 and CD81 [32,45], as well as exogenous markers reported to accumulate in LE/MVB ILVs; N-Rh-PE [37], indicate that WPB ILVs may represent a distinct population with similarities to those of platelet α-granules.

We looked for the presence of ESCRT components and associated proteins known to be involved in

MVB exosome formation and found syntenin localized to WPBs. Syntenin is a cytosolic PDZ domain protein that acts as an intracellular adapter involved in many processes including exosome biogenesis and secretion [51]. Syntenin binds directly to CD63 [52] and regulates formation of CD63-containing exosomes [51,53]. The localization of CD63 and syntenin on WPBs, the presence of cytoplasmic components within WPB ILVs may indicate formation of WPB ILVs by inward budding of the WPB limiting membrane during organelle maturation.

Growing evidence suggests that endothelial derived exosomes provide an important route for the exchange of proteins, lipids and nucleic acids that contribute to intercellular communication and regulation of the immune and cardiovascular systems [54,55]. Endothelial cell derived exosomes are reported to directly modulate many different target cells, [47,56,57], and in turn endothelial cells are a target for exosomes released from other cells [58-61]. For example, angiopoietin-2 (Ang2), an important regulator of vascular network formation, is secreted from endothelial cells on the outer surface of CD63-positive exosomes [47]. While the etiology of these secreted exosomes has been assumed to be LE/MVBs, Ang2 can be stored in the lumen of WPBs for regulated secretion [62], raising the intriguing possibility that some of these vesicles may be released through WPB exocytosis.

Endothelial cells accumulate hundreds of WPBs under resting conditions and may contain similar numbers of MVBs [1,21]. During Ca^{2+}-stimulation WPB exocytosis is rapid in onset, peaking 5-10 seconds after stimulation, involves up to 50% of the stored organelles and is largely complete within 1-2 minutes of stimulation [63]. Ca^{2+}-stimulated MVB fusion is reported to be slower in onset (2-6 minutes), involves a subpopulation of CD63+ MVBs [21,40,64] and is estimated to result in only a small fraction (~3%) of CD63+ MVB ILVs being released as exosomes [21]. WPBs are therefore well placed for exosome release following acute cell activation and prior to exosome release by MVB-fusion.

Addendum

J.S. A-V.F,J.T., N.I.K.,L.K.,T.C performed research and analyzed data; P.R. and T.C. designed the research; and wrote the paper. The authors report no disclosures.

Acknowledgements

The anti-CD63 monoclonal antibody H5C6 developed by August, J.T. and Hildreth, J.E.K. was obtained from the Developmental Studies Hybridoma Bank, created by the NICHD of the NIH and maintained at The University of Iowa, Department of Biology, Iowa City, IA 52242. TC was funded by the UK Medical Research Council under program grants MC_PC_13053. P.B.R. is supported by the Francis Crick Institute, which receives its core funding from Cancer Research UK (FC001156 and FC001143), the UK Medical Research Council (FC001156 and FC001143), and the Wellcome Trust (FC001156 and FC001143).

References

1. Schillemans M, Karampini E, Kat M, Bierings R. Exocytosis of Weibel-Palade bodies: how to unpack a vascular emergency kit. *J Thromb Haemost*. 2018;17(1):6-18.
2. Tkach M, Thery C. Communication by Extracellular Vesicles: Where We Are and Where We Need to Go. *Cell*. 2016;164(6):1226-1232.
3. Berriman JA, Li S, Hewlett LJ, et al. Structural organization of Weibel-Palade bodies revealed by cryo-EM of vitrified endothelial cells. *Proc Natl Acad Sci U S A*. 2009;106(41):17407-17412.
4. Sadler JE. von Willebrand factor assembly and secretion. *J Thromb Haemost*. 2009;7 Suppl 1:24-27.
5. Zhou YF, Eng ET, Nishida N, Lu C, Walz T, Springer TA. A pH-regulated dimeric bouquet in the structure of von Willebrand factor. *EMBO J*. 2011;30(19):4098-4111.
6. Doyle EL, Ridger V, Ferraro F, Turmaine M, Saftig P, Cutler DF. CD63 is an essential cofactor to leukocyte recruitment by endothelial P-selectin. *Blood*. 2011;118(15):4265-4273.
7. Poeter M, Brandherm I, Rossaint J, et al. Annexin A8 controls leukocyte recruitment to activated endothelial cells via cell surface delivery of CD63. *Nat Commun*. 2014;5:3738-.
8. Toothill VJ, Van Mourik JA, Niewenhuis HK, Metzelaar MJ, Pearson JD. Characterization of the enhanced adhesion of neutrophil leukocytes to thrombin-stimulated endothelial cells. *J Immunol*. 1990;145(1):283-291.
9. Kobayashi T, Vischer UM, Rosnoblet C, et al. The tetraspanin CD63/lamp3 cycles between endocytic and secretory compartments in human endothelial cells. *Mol Biol Cell*. 2000;11(5):1829-1843.
10. Harrison-Lavoie KJ, Michaux G, Hewlett L, et al. P-selectin and CD63 use different mechanisms for delivery to Weibel-Palade bodies. *Traffic*. 2006;7(6):647-662.
11. Marks MS, Heijnen HF, Raposo G. Lysosome-related organelles: unusual compartments become mainstream. *Curr Opin Cell Biol*. 2013;25(4):495-505.
12. Raposo G, Nijman HW, Stoorvogel W, et al. B lymphocytes secrete antigen-presenting vesicles. *J Exp Med*. 1996;183(3):1161-1172.
13. Raposo G, Marks MS, Cutler DF. Lysosome-related organelles: driving post-Golgi compartments into specialisation. *Curr Opin Cell Biol*. 2007;19(4):394-401.
14. Zografou S, Basagiannis D, Papafotika A, et al. A complete Rab screening reveals novel insights in Weibel-Palade body exocytosis. *J Cell Sci*. 2012;125(Pt 20):4780-4790.
15. Bierings R, Hellen N, Kiskin N, et al. The interplay between the Rab27A effectors Slp4-a and MyRIP controls hormone-evoked Weibel-Palade body exocytosis. *Blood*. 2012;120(13):2757-2767.
16. Nightingale TD, Pattni K, Hume AN, Seabra MC, Cutler DF. Rab27a and MyRIP regulate the amount and multimeric state of VWF released from endothelial cells. *Blood*. 2009;113(20):5010-5018.
17. van Breevoort D, Snijders AP, Hellen N, et al. STXBP1 promotes Weibel-Palade body exocytosis through its interaction with the Rab27A effector Slp4-a. *Blood*. 2014;123(20):3185-3194.
18. Heijnen HF, Schiel AE, Fijnheer R, Geuze HJ, Sixma JJ. Activated platelets release two types of membrane vesicles: microvesicles by surface shedding and exosomes derived from exocytosis of multivesicular bodies and alpha-granules. *Blood*. 1999;94(11):3791-3799.
19. Blanchard N, Lankar D, Faure F, et al. TCR activation of human T cells induces the production of exosomes bearing the TCR/CD3/zeta complex. *J Immunol*. 2002;168(7):3235-3241.
20. Ostrowski M, Carmo NB, Krumeich S, et al. Rab27a and Rab27b control different steps of the exosome secretion pathway. *Nat Cell Biol*. 2010;12(1):19-30; sup pp 11-13.
21. Messenger SW, Woo SS, Sun Z, Martin TFJ. A Ca(2+)-stimulated exosome release pathway in cancer cells is regulated by Munc13-4. *J Cell Biol*. 2018;217(8):2877-2890.
22. Meli A, Carter T, McCormack A, Hannah MJ, Rose ML. Antibody alone is not a stimulator of exocytosis of Weibel-Palade bodies from human endothelial cells. *Transplantation*. 2012;94(8):794-801.
23. Hewlett L, Zupancic G, Mashanov G, et al. Temperature-dependence of Weibel-Palade body exocytosis and cell surface dispersal of von Willebrand factor and its propolypeptide. *PLoS One*. 2011;6(11):e27314.
24. Mastronarde DN. Dual-axis tomography: an approach with alignment methods that preserve resolution. *J Struct Biol*. 1997;120(3):343-352.
25. Kiskin NI, Hellen N, Babich V, et al. Protein mobilities and P-selectin storage in Weibel-Palade bodies. *J Cell Sci*. 2010;123(Pt 17):2964-2975.
26. Kiskin NI, Babich V, Knipe L, Hannah MJ, Carter T. Differential cargo mobilisation within Weibel-Palade bodies after transient fusion with the plasma membrane. *PLoS One*. 2014;9(9):e108093.
27. Kowal J, Arras G, Colombo M, et al. Proteomic comparison defines novel markers to characterize heterogeneous populations of extracellular vesicle subtypes. *Proc Natl Acad Sci U S A*. 2016;113(8):E968-977.
28. Bobrie A, Colombo M, Krumeich S, Raposo G, Thery C. Diverse subpopulations of vesicles secreted by different intracellular mechanisms are present in exosome preparations obtained by differential ultracentrifugation. *J Extracell Vesicles*. 2012;1.
29. van Niel G, Charrin S, Simoes S, et al. The tetraspanin CD63 regulates ESCRT-independent and -dependent endosomal sorting during melanogenesis. *Dev Cell*. 2011;21(4):708-721.
30. Suetsugu A, Honma K, Saji S, Moriwaki H, Ochiya T, Hoffman RM. Imaging exosome transfer from breast

cancer cells to stroma at metastatic sites in orthotopic nude-mouse models. *Adv Drug Deliv Rev*. 2013;65(3):383-390.
31. Vischer UM, Wagner DD. CD63 is a component of Weibel-Palade bodies of human endothelial cells. *Blood*. 1993;82(4):1184-1191.
32. Escola JM, Kleijmeer MJ, Stoorvogel W, Griffith JM, Yoshie O, Geuze HJ. Selective enrichment of tetraspan proteins on the internal vesicles of multivesicular endosomes and on exosomes secreted by human B-lymphocytes. *J Biol Chem*. 1998;273(32):20121-20127.
33. Espenel C, Margeat E, Dosset P, et al. Single-molecule analysis of CD9 dynamics and partitioning reveals multiple modes of interaction in the tetraspanin web. *J Cell Biol*. 2008;182(4):765-776.
34. Colombo M, Raposo G, Thery C. Biogenesis, secretion, and intercellular interactions of exosomes and other extracellular vesicles. *Annu Rev Cell Dev Biol*. 2014;30:255-289.
35. Kobayashi T, Stang E, Fang KS, de Moerloose P, Parton RG, Gruenberg J. A lipid associated with the antiphospholipid syndrome regulates endosome structure and function. *Nature*. 1998;392(6672):193-197.
36. Wubbolts R, Leckie RS, Veenhuizen PT, et al. Proteomic and biochemical analyses of human B cell-derived exosomes. Potential implications for their function and multivesicular body formation. *J Biol Chem*. 2003;278(13):10963-10972.
37. Vidal M, Mangeat P, Hoekstra D. Aggregation reroutes molecules from a recycling to a vesicle-mediated secretion pathway during reticulocyte maturation. *J Cell Sci*. 1997;110 (Pt 16):1867-1877.
38. Willem J, ter Beest M, Scherphof G, Hoekstra D. A non-exchangeable fluorescent phospholipid analog as a membrane traffic marker of the endocytic pathway. *Eur J Cell Biol*. 1990;53(1):173-184.
39. MacKenzie A, Wilson HL, Kiss-Toth E, Dower SK, North RA, Surprenant A. Rapid secretion of interleukin-1beta by microvesicle shedding. *Immunity*. 2001;15(5):825-835.
40. Verweij FJ, Bebelman MP, Jimenez CR, et al. Quantifying exosome secretion from single cells reveals a modulatory role for GPCR signaling. *J Cell Biol*. 2018;217(3):1129-1142.
41. Edgar JR, Manna PT, Nishimura S, Banting G, Robinson MS. Tetherin is an exosomal tether. *Elife*. 2016;5.
42. Babich V, Meli A, Knipe L, et al. Selective release of molecules from Weibel-Palade bodies during a lingering kiss. *Blood*. 2008;111(11):5282-5290.
43. Zenner HL, Collinson LM, Michaux G, Cutler DF. High-pressure freezing provides insights into Weibel-Palade body biogenesis. *J Cell Sci*. 2007;120(Pt 12):2117-2125.
44. Valentijn KM, van Driel LF, Mourik MJ, et al. Multigranular exocytosis of Weibel-Palade bodies in vascular endothelial cells. *Blood*. 2010;116(10):1807-1816.
45. Pols MS, Klumperman J. Trafficking and function of the tetraspanin CD63. *Exp Cell Res*. 2009;315(9):1584-1592.
46. Kowal J, Tkach M, Thery C. Biogenesis and secretion of exosomes. *Curr Opin Cell Biol*. 2014;29:116-125.
47. Ju R, Zhuang ZW, Zhang J, et al. Angiopoietin-2 secretion by endothelial cell exosomes: regulation by the phosphatidylinositol 3-kinase (PI3K)/Akt/endothelial nitric oxide synthase (eNOS) and syndecan-4/syntenin pathways. *J Biol Chem*. 2014;289(1):510-519.
48. Theos AC, Tenza D, Martina JA, et al. Functions of adaptor protein (AP)-3 and AP-1 in tyrosinase sorting from endosomes to melanosomes. *Mol Biol Cell*. 2005;16(11):5356-5372.
49. Peden AA, Oorschot V, Hesser BA, Austin CD, Scheller RH, Klumperman J. Localization of the AP-3 adaptor complex defines a novel endosomal exit site for lysosomal membrane proteins. *J Cell Biol*. 2004;164(7):1065-1076.
50. Luzio JP, Pryor PR, Bright NA. Lysosomes: fusion and function. *Nat Rev Mol Cell Biol*. 2007;8(8):622-632.
51. Baietti MF, Zhang Z, Mortier E, et al. Syndecan-syntenin-ALIX regulates the biogenesis of exosomes. *Nat Cell Biol*. 2012;14(7):677-685.
52. Latysheva N, Muratov G, Rajesh S, et al. Syntenin-1 is a new component of tetraspanin-enriched microdomains: mechanisms and consequences of the interaction of syntenin-1 with CD63. *Mol Cell Biol*. 2006;26(20):7707-7718.
53. Friand V, David G, Zimmermann P. Syntenin and syndecan in the biogenesis of exosomes. *Biol Cell*. 2015;107(10):331-341.
54. Dignat-George F, Boulanger CM. The many faces of endothelial microparticles. *Arterioscler Thromb Vasc Biol*. 2011;31(1):27-33.
55. Sluijter JP, Verhage V, Deddens JC, van den Akker F, Doevendans PA. Microvesicles and exosomes for intracardiac communication. *Cardiovasc Res*. 2014;102(2):302-311.
56. Sheldon H, Heikamp E, Turley H, et al. New mechanism for Notch signaling to endothelium at a distance by Delta-like 4 incorporation into exosomes. *Blood*. 2010;116(13):2385-2394.
57. Hergenreider E, Heydt S, Treguer K, et al. Atheroprotective communication between endothelial cells and smooth muscle cells through miRNAs. *Nat Cell Biol*. 2012;14(3):249-256.
58. Al-Nedawi K, Szemraj J, Cierniewski CS. Mast cell-derived exosomes activate endothelial cells to secrete plasminogen activator inhibitor type 1. *Arterioscler Thromb Vasc Biol*. 2005;25(8):1744-1749.
59. Umezu T, Ohyashiki K, Kuroda M, Ohyashiki JH. Leukemia cell to endothelial cell communication via exosomal miRNAs. *Oncogene*. 2013;32(22):2747-2755.
60. Gambim MH, do Carmo Ade O, Marti L, Verissimo-Filho S, Lopes LR, Janiszewski M. Platelet-derived exosomes induce endothelial cell apoptosis through peroxynitrite generation: experimental evidence for a novel mechanism of septic vascular dysfunction. *Crit Care*. 2007;11(5):R107.

61. Lee HD, Kim YH, Kim DS. Exosomes derived from human macrophages suppress endothelial cell migration by controlling integrin trafficking. *Eur J Immunol*. 2014;44(4):1156-1169.
62. Fiedler U, Scharpfenecker M, Koidl S, et al. The Tie-2 ligand angiopoietin-2 is stored in and rapidly released upon stimulation from endothelial cell Weibel-Palade bodies. *Blood*. 2004;103(11):4150-4156.
63. Erent M, Meli A, Moisoi N, et al. Rate, extent and concentration dependence of histamine-evoked Weibel-Palade body exocytosis determined from individual fusion events in human endothelial cells. *J Physiol*. 2007;583(Pt 1):195-212.
64. Savina A, Furlan M, Vidal M, Colombo MI. Exosome release is regulated by a calcium-dependent mechanism in K562 cells. *J Biol Chem*. 2003;278(22):20083-20090.

Figures

Figure 1

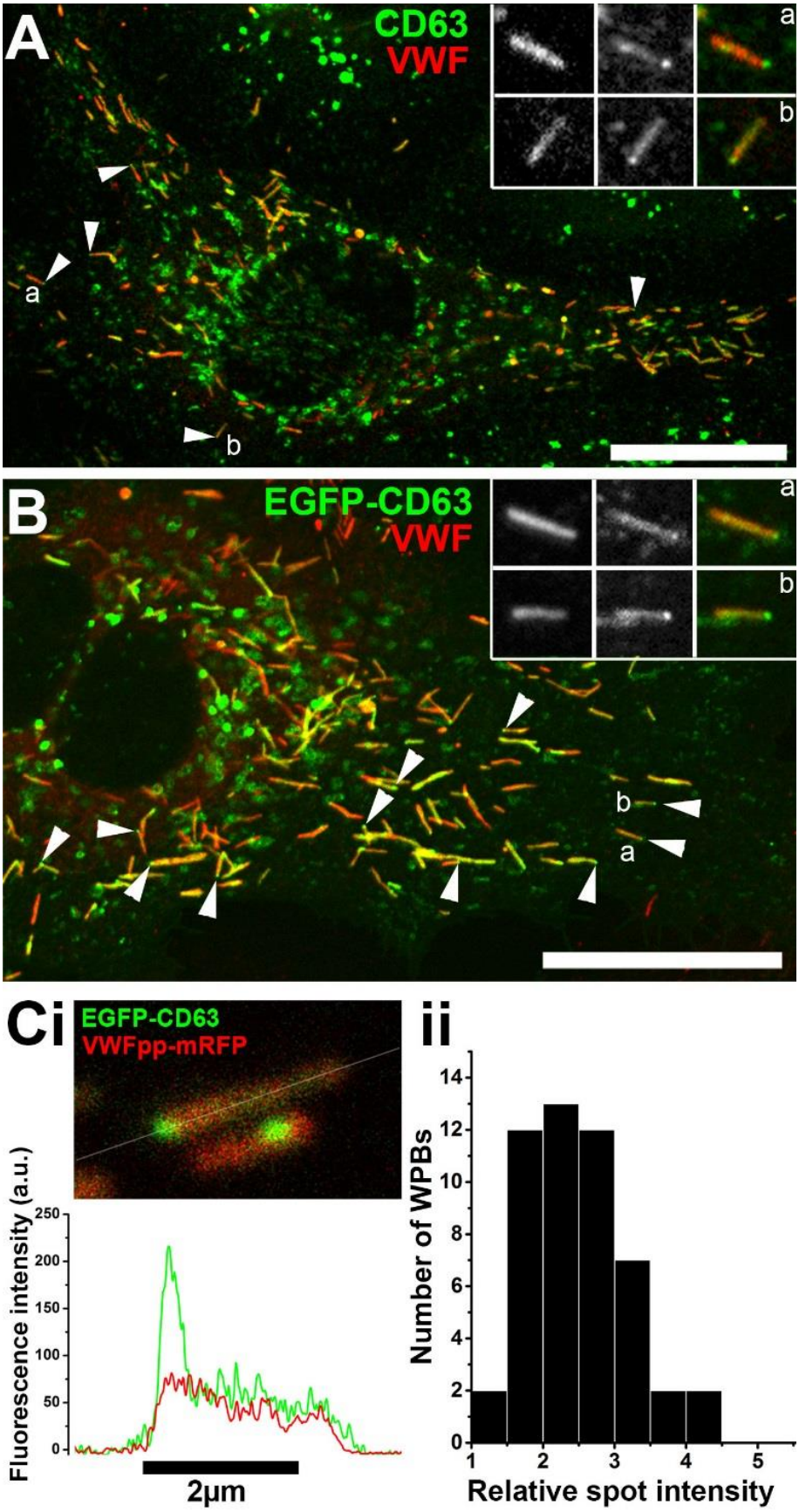

Figure 1. CD63 is enriched in micro domains on WPBs.

A-B; Confocal images of single fixed HUVEC (A) immuno-labelled with specific antibodies to CD63 (green) and VWF (red) or (B) expressing exogenous EGFP-CD63 (green) and immuno-labelled for VWF (red). Scale bars are 10µm. Arrow heads indicate bright regions of CD63 (A) or EGFP-CD63 (B) closely associated with individual WPBs. Inset panels show on expanded scales the fluorescence, in grey scale, for VWF (left) and CD63 (middle) and the colour merge image (right; VWF in red, CD63 in green) for WPBs indicated by a and b. Images A and B were taken at room temperature using a Leica SP2 confocal microscope and software (Mannheim, Germany) equipped with a PL APO100x 1.4NA objective. (Ci) Image from a live cell confocal fluorescence experiment of an EGFP-CD63 (green) and VWFpp-mRFP (red) co-expressing HUVEC showing two WPBs containing discrete bright micro-domains of EGFP-CD63 fluorescence. Intensity plots through the long axis of the upper WPB (white line) are shown below (green: CD63, red VWFpp). (Cii) Histogram of the fold increase in mean EGFP fluorescence intensity in micro-domains compared to non-micro-domain regions (bulk WPB membrane) for 50 WPBs. Mean micro-domain EGFP intensity was 2.5±0.7 fold (n=49 WPbs, range 1.4-4.1) that in the bulk membrane of the corresponding WPB. Images in C were taken at 37°C using a Leica SP5 with a HCX PL APO CS 100.0x 1.46NA Oil objective, pinhole (airy) 1.5, zoom 30-35.5, scan speed 1400Hz in xyt acquisition mode.

Figure 2

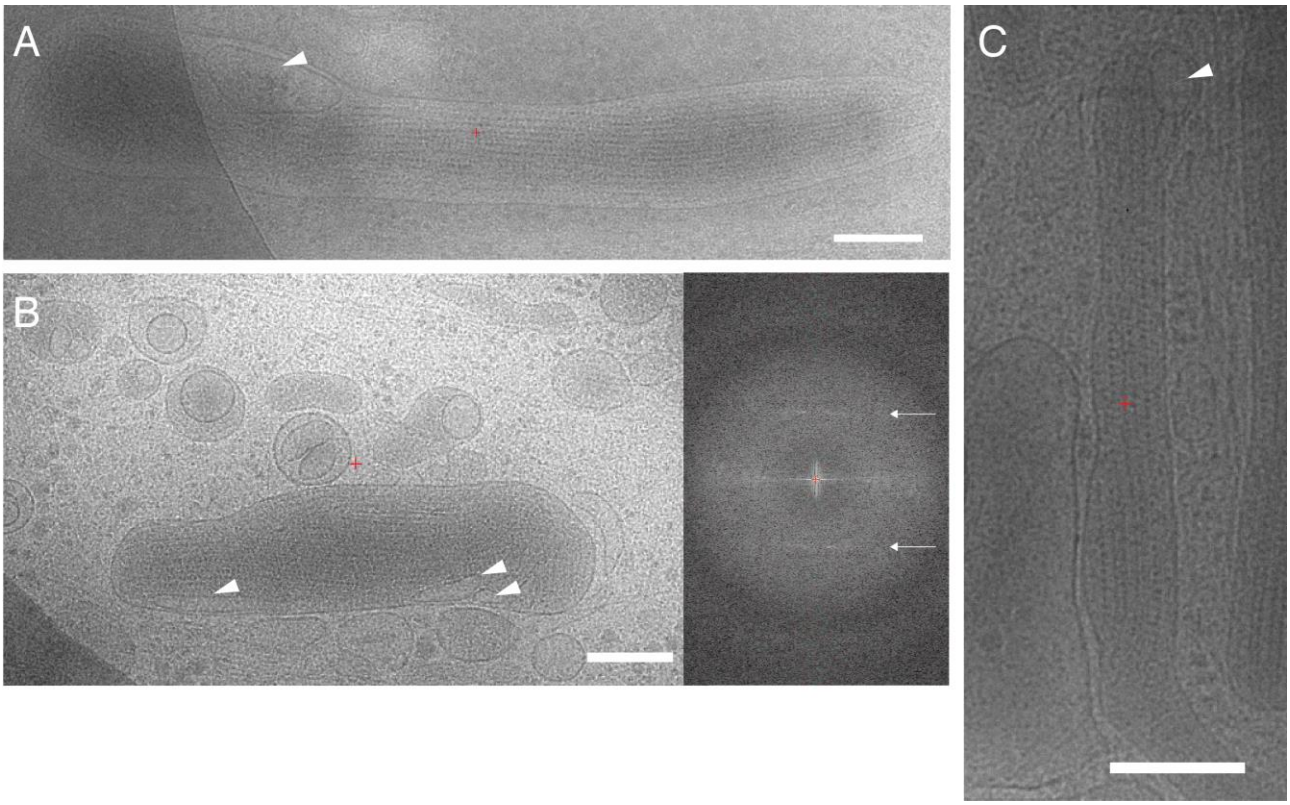

Figure 2. Electron cryomicroscopy of frozen-hydrated HUVECs showing Weibel-Palade Bodies in cytoplasm.

A-C 2D images of Weibel-Palade Bodies show internal density for VWF tubules. ILVs are indicated by triangular white arrows. Fourier transform of WPB interior in B shows helical layer lines for VWF (arrows). Scale bars are 200 nm.

Figure 3

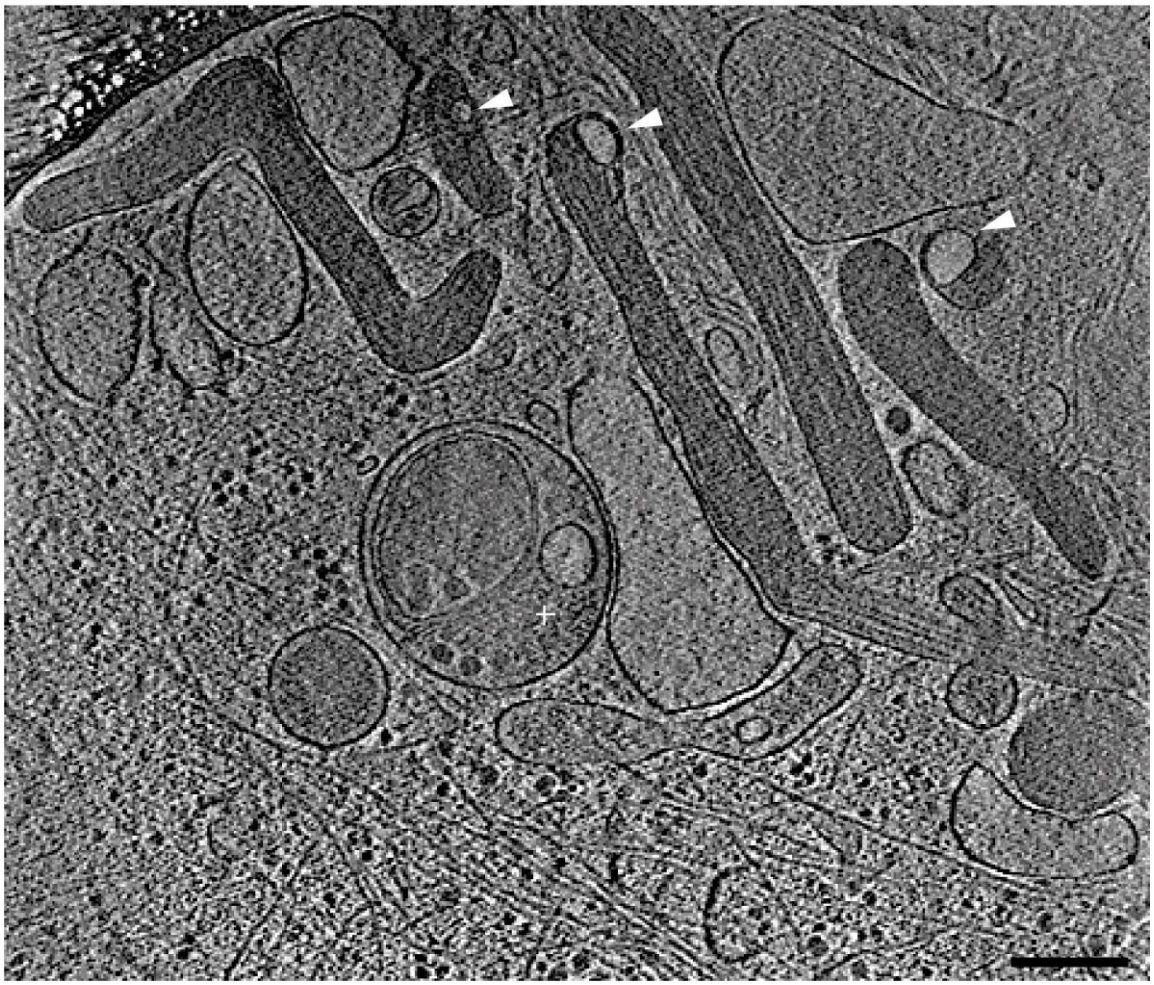

Figure 3. Section of an electron cryotomogram of a frozen-hydrated endothelial cell showing region with Weibel-Plade bodies. ILV's within Weibel-Palade bodies indicated by arrow. Scale bar is 200 nm.

Figure 4

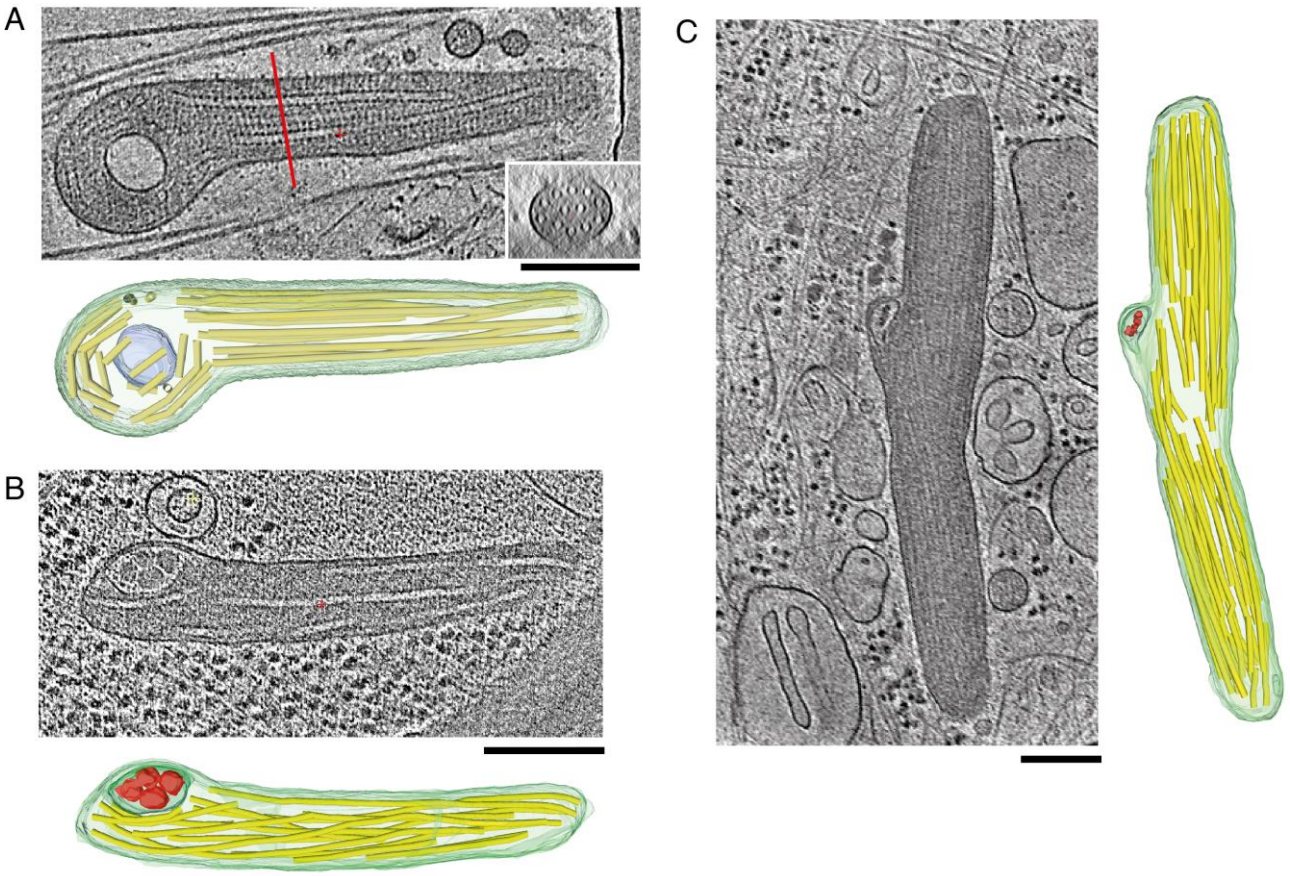

Figure. 4. Tomogram sections of Weibel-Palade bodies containing ILVs along with structural models.

Tomogram section with structural model consisting of WPB limiting model green, ILV membrane blue-green, VWF tubules yellow, and ILV internal content, red. (A) inset shows tomogram cross-section at location of red line. (B) WPB from an HHMEC with an ILV at the left side of the granule. The ILV contains internal content similar to cytoplasmic granules as shown in Supplementary Figure S4. (C) WPB in a HUVEC with kink in the middle where tubules have disrupted the paracrystalline order. The ILV contains density similar in size to cytosolic densities visible throughout tomogram section. Scale bars are 200 nm.

Figure 5

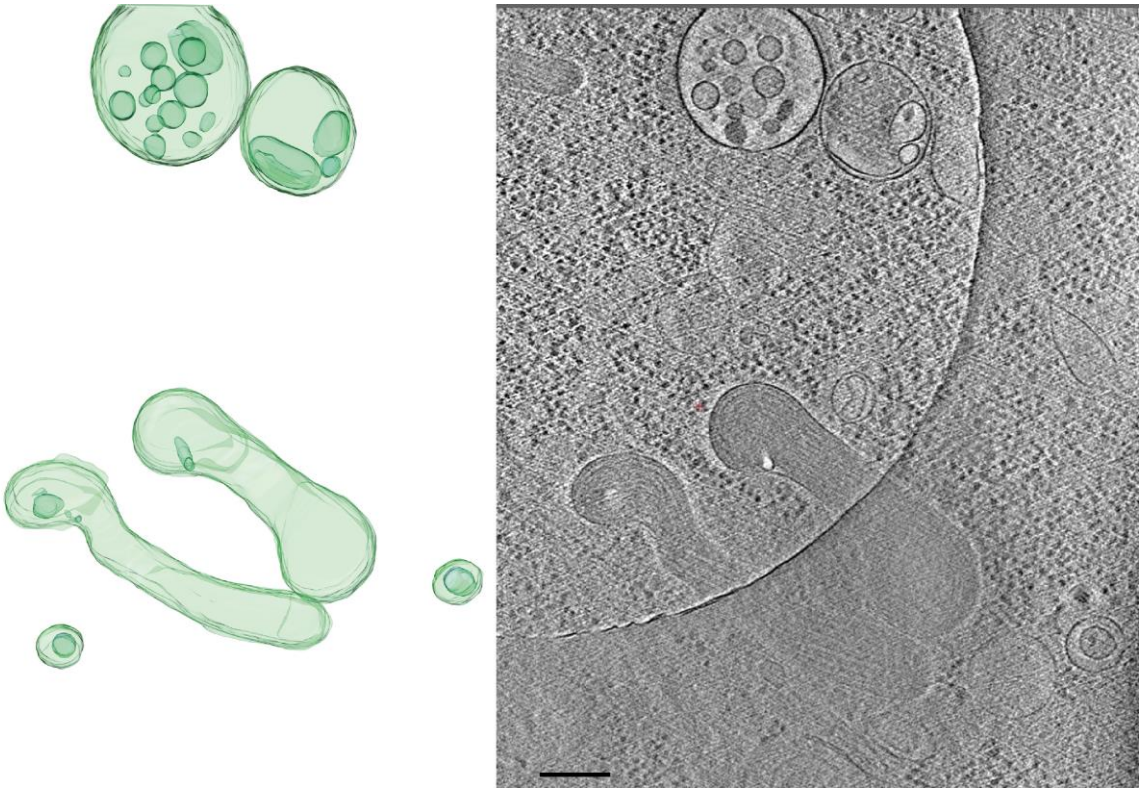

Figure 5. Tomogram section showing WPBs and MVBs.

Tomogram section (right) shows WPBs and MVBs containing ILVs as indicated in structural model (left).

Figure 6

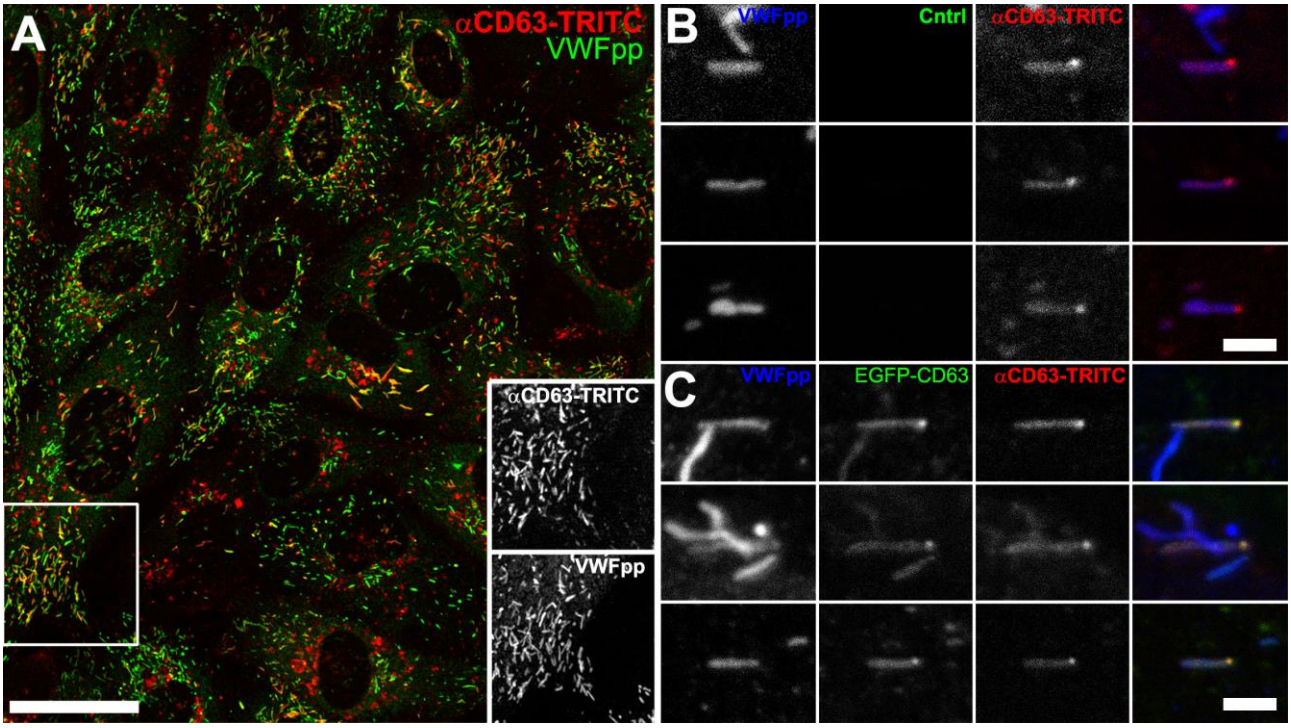

Figure 6 CD63 in WPB ILVs is of endosomal origin. (A) confocal fluorescence image of HUVEC incubated live in the presence of an extracellular TRITC-conjugated mouse anti-CD63 antibody (red; 1:55 dilution, 24 h). The cells were fixed and immunolabelled with a specific antibody to VWFpp (green). Scale bar 20µm. The region indicated by the white box is shown as grey scale inserts to illustrate the accumulation of extracellular applied TRITC-anti-CD63 in WPBs. (B-C) examples of the accumulation of extracellular applied TRITC-anti-CD63 in micro-domains in WPBs in control (B; mock transfected) or EGFP-CD63 transfected (C) HUVEC incubated live with the TRITC-anti-CD63 (red) and subsequently immunolabelled for VWFpp (blue) and EGFP-CD63 (anti-GFP antibody, green). TRITC-anti-CD63 can be seen in bright micro-domains on WPBs that co-localised with EGFP-CD63 micro-domains. Scale bars 2µm.

Figure 7

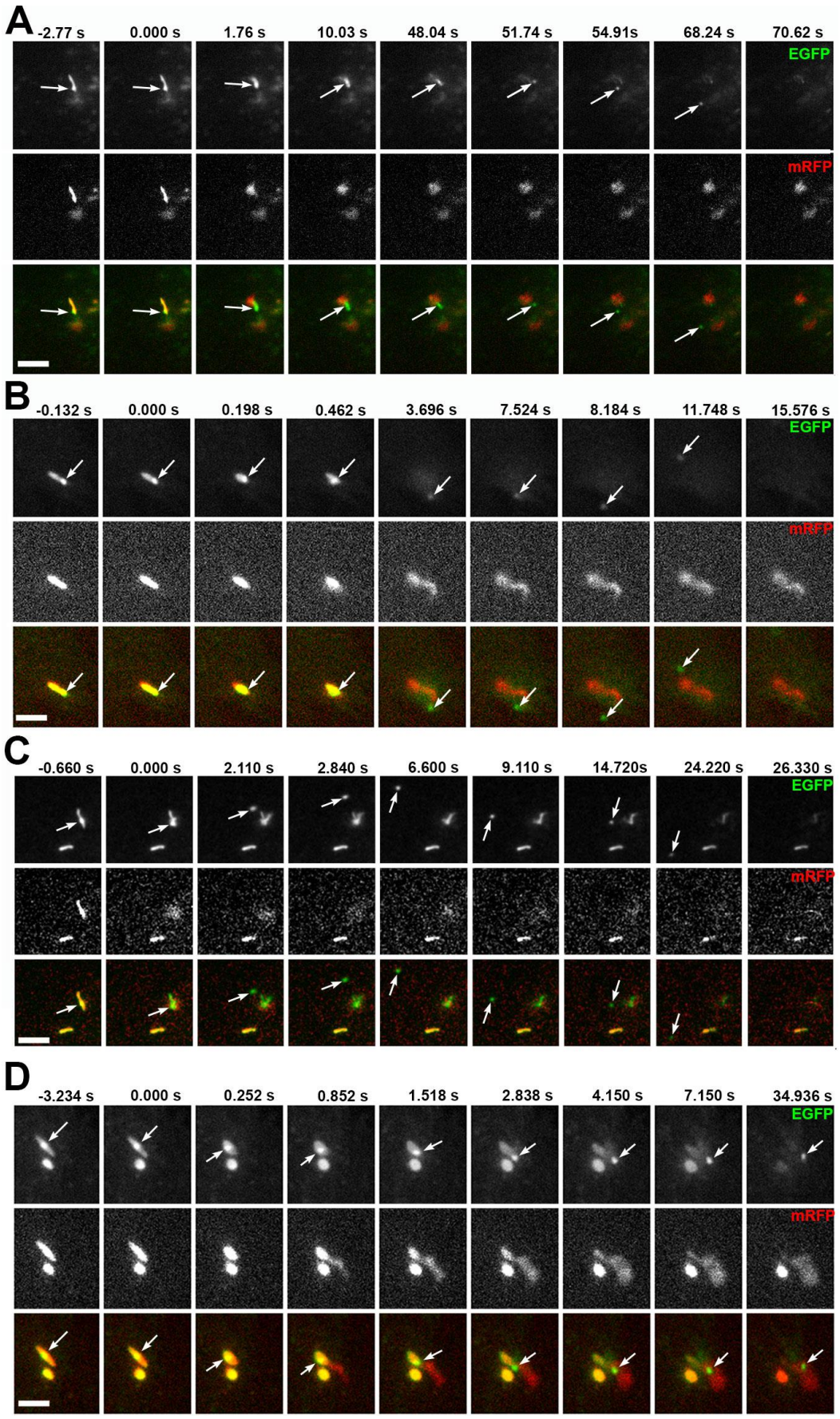
A
-2.77 s
0.000 s
1.76 s
10.03 s
48.04 s
51.74 s
54.91s
68.24 s
70.62 s
EGFP
mRFP
B
-0.132 s
0.000 s
0.198 s
0.462 s
3.696 s
7.524 s
8.184 s
11.748 s
15.576 s
EGFP
mRFP
C
-0.660 s
0.000 s
2.110 s
2.840 s
6.600 s
9.110 s
14.720s
24.220 s
26.330 s
EGFP
mRFP
D
-3.234 s
0.000 s
0.252 s
0.852 s
1.518 s
2.838 s
4.150 s
7.150 s
34.936 s
EGFP
mRFP

Figure. 7. WPB EGFP-CD63 micro-domains are secreted as discrete particles during exocytosis. A-D show examples of image montages taken from dual colour live cell videos (Supplementary videos S8, S9, S10 and S11 respectively) of EGFP-CD63 (top panels, green in colour merge) and VWFpp-mRFP (middle panels) containing WPBs prior to (frame 1) and during (frames 2-9) exocytosis evoked by histamine stimulation (100µM). Scale bars are 2µm. In each case the WPB indicated by the arrow undergoes a morphological transition from rod to spheroid shape accompanied by expulsion of VWFpp-EGFP and release of the EGFP-CD63 ILV as a discrete particle. In examples A-C the EGFP-CD63 particle diffuses out of the field of view, in D the particle remains trapped within the patch of secreted VWF. Images were acquired sequentially on a wide field microscope equipped with an Olympus UPLSAPO 100x 1.4NA objective, OptoLED epifluorescence excitation system and Andor Ixon3 EMCCD camera operating at 30 frames per second.

Stimulated release of intraluminal vesicles from Weibel-Palade Bodies

James Streetley[1† ‡], Ana-Violeta Fonseca[1‡], Jack Turner[2] Nikolai I. Kiskin[1¶], Laura Knipe[1#], Peter B. Rosenthal[1,2], Tom Carter[1,3]

[1]MRC National Institute for Medical Research, The Ridgeway, London NW7 1AA [2]Structural Biology of Cells and Viruses Laboratory, The Francis Crick Institute, 1 Midland Road, London NW1 1AT. [3]Molecular and Clinical Sciences Research Institute, St George's University, London, SW17 0RE.

Present addresses: [†]J.S., MRC-University of Glasgow Centre for Virus Research, Sir Michael Stoker Building, 464 Bearsden Road, Glasgow, G61 1QH. [¶]N.I.K., Flat 15 Holmdene, Holden Road, London N12 8HU. [#]L.K.,The Francis Crick Institute, 1 Midland Road, London NW1 1AT.

[‡]These authors contributed equally.

Running head: Intra-luminal vesicles of WPBs

Corresponding Authors: Prof. Tom. Carter,
Molecular and Clinical Sciences Research Institute,
St George's University,
London,
SW17 0RE
tcarter@sgul.ac.uk

Dr. Peter B. Rosenthal,
Structural Biology of Cells and Viruses Laboratory
The Francis Crick Institute
1 Midland Road,
London NW1 1AT
Peter.Rosenthal@crick.ac.uk

Category: Regular article

Abstract:	159
Main text:	3962
Figures:	7
Refs:	64

Key Points:

- Weibel-Palade bodies (WPBs) contain CD63-positive intraluminal vesicles that are released during secretagogue-evoked exocytosis.
- Cryo-electron microscopy of intact vitrified endothelial cells reveal intraluminal vesicles as a novel structural feature of WPBs.

Abstract

Weibel-Palade bodies (WPBs) are secretory granules that contain von Willebrand factor and P-selectin, molecules that regulate hemostasis and inflammation respectively. The presence of CD63/LAMP3 in the limiting membrane of WPBs has led to their classification as lysosome-related organelles. Many lysosome-related organelles contain intraluminal vesicles (ILVs) enriched in CD63 that are secreted into the extracellular environment during cell activation to mediate intercellular communication. To date there are no reports that WPBs contain or release ILVs. By light microscopy and live-cell imaging we show that CD63 is enriched in micro-domains within WPBs. Extracellular antibody recycling studies showed that CD63 in WPB micro-domains can originate from the plasma membrane. By cryo-electron tomography of frozen-hydrated endothelial cells we identify internal vesicles as a novel structural feature of the WPB lumen. By live-cell fluorescence microscopy we observe directly the exocytotic release of EGFP-CD63 ILVs as discrete particles from individual WPBs. WPB exocytosis provides a novel route for release of ILVs during endothelial cell stimulation.

Key Words: electron cryomicroscopy, endothelial cells, Weibel-Palade body, intra-luminal vesicle, von Willebrand factor, exosome, CD63, P-selectin.

Introduction

Endothelial cells regulate hemostasis and inflammation through direct cell-cell contacts, secretion of soluble or membrane associated mediators, and through the release of small bioactive lipid vesicles (extracellular vesicles; EVs). Many of the soluble secreted molecules, such as the adhesive glycoprotein von Willebrand Factor, are stored and released in a regulated fashion from specialized secretory granules called Weibel-Palade bodies (WPBs) [1]. EVs can arise by several distinct mechanisms: (1) exocytosis of late endosomes/multivesicular bodies (LE/MVBs) to release intra-luminal vesicles (ILVs; termed exosomes upon secretion) (2) budding from the plasma membrane (shedding micro-vesicles or ecotosomes), or (3) plasma membrane blebbing during programmed cell death (apoptotic bodies). EVs contain a variety of signaling molecules that modulate gene expression and function of target cells, and are now widely viewed as important mediators of intercellular communication and control [2].

WPBs form at the trans-Golgi network (TGN) through a pH- and Ca^{2+}-dependent condensation of von Willebrand factor (VWF) and the VWF-propolypeptide (VWFpp) to form helical tubule structures [3-5]. VWF-VWFpp tubules comprise the majority of the protein content of WPBs and give the organelle its distinctive morphology [3]. The leukocyte adhesion molecule P-selectin is also stored in the WPB limiting membrane and upon release into the plasma membrane it mediates the tethering and rolling of leukocytes on the vessel wall prior to extravasation at sites of inflammation. Efficient P-selectin-mediated leukocyte capture requires the tetraspanin CD63 (also called LAMP3) that is also present in the limiting membrane of WPBs and co-released to the plasma membrane during exocytosis [6-8]. P-selectin enters WPBs during their formation at the TGN, however, CD63 is delivered to WPBs at a later stage through a poorly defined interaction with LE\MVBs [9,10] requiring the endosomal sorting complex AP-3 and annexin 8 [7,10].

The interaction of WPBs with endosomal components, their acidic lumenal pH, and acquisition of CD63/LAMP3 have led to the WPBs classification as a lysosomal-related organelle (LRO) [11], a

functionally diverse set of compartments containing different cargoes that none-the-less share certain features or components with lysosomes. LRO biogenesis is complex and organelle-specific: Some form by re-modeling/maturation of endosomal compartments (e.g. MVBs, secretory lysosomes, melanosomes), some originate from the TGN (WPBs), while others may involve contributions from both pathways (e.g. lytic granules, platelet granules) [11].

LROs that undergo fusion with the plasma membrane to release their contents include the major histo-compatibility complex class II-enriched compartment of B lymphocytes, lytic granules of cytotoxic T cells, platelet dense core and α-granules, basophilic granules, lamellar bodies of lung epithelia cells, osteoclast granules, sperm acrosomes and WPBs [12,13]. In most cases the delivery of these organelles to the plasma membrane, and their exocytosis, is regulated by "secretory Rab proteins" and their effector molecules. For WPBs, these include Rab27A, MyRIP, Slp4-a and Munc13-4 [14-17]. Some LRO's contain ILVs that can be released during fusion with the plasma membrane [12,18,19], and unsurprisingly several key regulators of WPB and other LRO exocytosis (e.g. Rab27A, Slp4-a) also control exosome release [20,21]. Despite their classification as LROs and sharing a common set of molecular components regulating exocytosis, it is not known whether WPBs contain or release ILVs. Using live-cell imaging and high-resolution cryo-EM tomography of vitrified endothelial cells we identify and characterize ILVs in WPBs. We directly demonstrate the exocytotic release of EGFP-CD63 enriched ILVs from individual WPBs during hormone-stimulation. This is a new route for EV release from endothelial cells and extends the range of signaling modalities through WPBs.

Methods

Endothelial cell culture, transfections, immunocytochemistry, antibodies, DNA constructs and reagents

Human umbilical vein endothelial cells (HUVEC) or human heart microvasculature endothelial cells (HHMEC) were purchased, cultured, Nucleofected and processed for immunocytochemistry as previously described [15,22]. VWF-mRFP or -mCherry, VWFpp-mRFP, VWFpp-mEGFP, mRFP-Rab27A and EGFP-CD63 have been described previously (see [15] and references therein). Rabbit anti-VWF (A0082, 1:10000 dilution) was from Dako Ltd (Ely, UK), rabbit anti-VWFpp (1:500) is described in [23], mouse anti-LBPA (Z-PLBPA, 1:1000) was from Tebu-bio (Peterborough, UK), mouse anti-P-selectin (clone AK6, 1:50) was from Serotec (Kidlington, UK), rabbit anti-VPS2B (ab33174, 1:300) and mouse anti-Alix (ab117600, 1;300) were from Abcam (Cambridge, UK), rabbit anti-syntenin (133003, 1:100) was from Synaptic Systems GmbH (Gottingen, DE), mouse anti-TSG101 (GTX70255) and rat anti-HSP70 (GTX191366) were from GeneTex (Irvine, CA), mouse anti-CD9 (clone HI9a, 1:1000), anti-CD81 (clone 5A6, 1;1000) were from Biolegend (London, UK), mouse anti-CD63 (clone H5C6, 1;200) was from the Developmental Studies Hybridoma Bank (see Acknowledgments), normal mouse IgG_1 (SC-3877, 1;55) and mouse anti-CD63-TRITC (SC-5275, 1:55) were from Insight Biotechnology ltd (Wembly, UK), from Abcam. Secondary antibodies coupled to fluorophores (1:200) were from Jackson Immunoresearch (USA). All other reagents were from Sigma-Aldrich unless otherwise stated.

Cell culture on electron microscopy grids, electron cryomicroscopy and image and tilt series and tomogram analysis.

HUVEC or HHMEC were grown on carbon film on gold grid supports for microscopy as previously described [3]. Gold grids with cells on were washed briefly in PBS and 4 µl of 40% protein A conjugated 10nm gold colloid (BBI Life Sciences) in PBS added between washing and freezing, to act as fiducial markers. WPBs were imaged in cells either unstimulated or following

stimulation. For stimulation PBS contained 100 µM histamine dihydrochloride or ionomycin (300nM or 1 µM ionomycin, Streptomyces conglobatus).

Grids were frozen by plunging into liquid ethane using either a manual plunge-freezer or an FEI Vitrobot Mark III (FEI Company) at either at room temperature and humidity (manual) or at 22°C and room humidity (Vitribot; humidifier switched to off). Frozen grids were stored in liquid N_2. Frozen grids were imaged using either a Spirit TWIN microscope (FEI) operating at 120 kV and equipped with an Eagle 2k camera (FEI) using a Gatan 626 cryotomography holder or a LN_2 cooled Polara microscope (FEI) operating at 200 kV and equipped with a F224 CCD camera (TVIPS). Both TIA (FEI) and SerialEM [63] image acquisition software were used, and low-dose procedures were used in both packages. SerialEM was used to collect whole grid montages at ~140x magnification, which were used for locating areas of interest for further imaging using low-dose procedures.

Single-axis tilt-series were collected automatically using SerialEM, with an angular range of -60° to +60° and increment of 2° or 3°. Total dose for tilt-series were limited to 50 to 70 e^-/A^2, giving individual images with a dose of 1.2 to 1.7 e^-/A^2. The dose per image was kept constant for each tilt angle in a series. The target defocus was set at -8 µm. Tomographic tilt series were aligned using fiducials using Etomo from the in IMOD software [24]. Projection images in aligned tilt series were normalized based on their histograms and reconstructed to 3D volumes and analyzed as previously described [3].

Image and volume analysis.

Simple image processing tasks such as crop, pad and rotate were performed in Ximdisp and FFT calculations were performed using Ximdisp and _trans from the MRC suite. Figures were prepared using Photoshop CS4 (Adobe). Amira (FEI Visualization Sciences Group), and IMOD were used to generate 3D models.

VWF tubules were manually traced using IMOD. Tomograms were segmented using the Amira 'Segmentation' tool. Membranes and tubules were rendered and displayed in Amira.

Live cell fluorescence imaging, confocal FRAP and analysis.

Nucleofected cells were plated at confluent density in culture medium onto 35 mm diameter poly d-lysine coated glass glass-bottomed culture dishes (MatTeK corp. Ashland, USA) or 25 mm diameter glass coverslips (#1.0, 0.15 mm, VWR International, UK). 25 mm diameter glass coverslips were mounted in Rose chambers containing physiological saline (in mM): NaCl- 140, KCl- 5, $MgSO_4$- 1, $CaCl_2$- 2, Glucose- 10, HEPES- 20, pH 7.3 (adjusted with NaOH). High speed dual-color epifluorescence imaging was carried out on an Olympus IX71 inverted microscope equipped with an Olympus UPLSAPO x100 oil 1.40NA objective, a 1.6x magnifier and an Ixon3 EMCCD camera operated in frame transfer mode at full gain and cooled to –70ºC (Andor, Belfast, United Kingdom). Full frame images were acquired at 30 frames s^{-1}. High-speed single or sequential dual color excitation wavelength switching (470±40nm and 572±35nm) was by OptoLED (Cairn Research, Faversham, UK), the excitation filter set comprising a GFP/DsRed dual band dichrochic mirror (Chroma part 51019) and a GFP/DsRed dual band emitter. Image capture and wavelength switching was synchronized using WinFluor software (Dr John Dempster, Strathclyde University, Glasgow, United Kingdom). The microscope was housed within an environmental chamber maintained at 36ºC and cells stimulated with histamine (100µM). Confocal FRAP experiments were carried out using Leica Microsystems TCS SP2 or SP5 (8 kHz resonant scanner) confocal microscopes equipped with Leica HCX PL APO x63 1.32NA (SP2) or HCX PLAPO CS x100 oil-immersion objectives with NA of 1.40 (SP2) or 1.46 (SP5) as previously described [15,25,26]. Excitation (bidirectional "fly" FRAP mode) was at 488nm (EGFP) and 561nm (mRFP). Emission windows for single-wavelength (EGFP) were 495-620nm and for dual-colour (EGFP, mRFP; simultaneous "fly" mode excitation) were, EGFP;500-545 nm, mRFP;585-750nm. Images from SP2 were collected at 512x128 (or 64) pixels and at zooms 20-32, and from SP5 at 512x300 pixels at zooms between 19.1 and 38.8. FRAP imaging

and ROIs were set as previously described [15,25,26] and single or dual-color bleaching applied during 2-10 consecutive frames acquired at 0.344 seconds (SP2) and between 0.792 and 0.962 was seconds (SP5). Images were background-subtracted and analyzed using custom-made macros implemented in ImageJ (http://rsb.info.nih.gov/ij/) [26]. Image montages and AVI video clips (Jpeg compression) were made in ImageJ2\Fiji. Data plots were made in Origin 9.2 (OriginLab Corporation, Northampton, USA). Results are expressed as mean ± s.e.m.

Results

Enrichment of CD63 in discrete micro-domains within WPBs

Tetraspanins, including the ubiquitously expressed CD63, are amongst the most common endosomal components enriched in secreted ILVs [27,28] (http://www.exocarta.org/), and CD63 in particular is implicated in cargo sorting to exosomes [29]. Consequently CD63 is widely used as a marker to identify, visualize and track ILVs/exosomes within and between cells [30]. To determine if WPBs contained CD63-enriched regions we first analyzed the pattern of endogenous CD63 in WPBs by immunocytochemistry (Figure 1A). Consistent with previous studies CD63-immunoreactivity was seen on both WPBs and other endomembrane compartments [31]. Close inspection revealed discrete bright "micro-domains" of CD63-immunoreactivity associated with some WPBs, often near the ends of the organelle but also at intermediate points up to mid-body (Supplementary Figure S1A). Expression of EGFP-CD63 produced similar features (Figure 1B), and crucially, live-cell fluorescence imaging showed that the EGFP-CD63 micro-domains were connected to and moved with (but not within) the WPB (See Supplementary videos S1 and S2). Measurement of WPB EGFP-CD63 fluorescence intensity in live cells showed the micro-domains to be stable in intensity and up to 4-5 times brighter than the bulk signal in the WPB membrane (Figure 1C), reminiscent of the enrichment reported for CD63 in ILVs of LE/MVBs and exosomes [32]. Further immunofluorescence analysis showed that other WPB membrane proteins (Rab27A, P-selectin) were present in the limiting membrane of the granule but were not concentrated in CD63-rich micro-domains (Supplementary Figure S1B).

At the plasma membrane, tetraspanins can form enriched areas or microdomains that appear as long-lived "spot-like" structures in which contributing tetraspanins, and associated proteins, are in dynamic exchange with the bulk plasma membrane on a time scale of seconds [33]. To examine if EGFP-CD63 in the WPB limiting membrane was in diffusional equilibrium with CD63 microdomains we used single WPB FRAP analysis in EGFP-CD63 and VWF-mRFP co-expressing HUVEC [25,26] Consistent with our previous studies[25] EGFP-CD63 was freely mobile in the WPB limiting membrane,

undergoing rapid and complete recovery, by lateral membrane diffusion, after each period of bleaching (Supplementary Figure S2, and Supplementary video S3). The core protein VWF-mRFP was used to confirm the organelle's identity, and was completely immobile showing no recovery after bleaching, as previously reported [25]. Our FRAP analysis showed that EGFP-CD63 in micro domains did not contribute to recovery of EGFP-CD63 fluorescence within the limiting membrane nor did micro domains re-accumulate fluorescence from the WPB limiting membrane when selectively bleached (Supplementary Figure S2). The results indicate that EGFP-CD63 in microdomains is not in diffusional equilibrium with EGFP-CD63 in the WPB limiting membrane.

Intra-luminal vesicles in WPBs revealed by cryo-electron tomography

The presence of micro-domains containing the membrane tetraspanin CD63 but topologically separated from the WPB membrane suggested that these were ILVs. To test this we applied high-resolution electron cryomicroscopy to image the thin edge of plunge-frozen, whole mount HUVECs, an approach that we have previously shown to reveal the high-resolution architecture of organelles without chemical fixation or staining [3]. In 2D projection images, WPBs appear as rod-shaped granules denser than the surrounding cytoplasm (Figure 2A-C) containing tubules of VWF which are the source of the signature helical pattern in their Fourier transforms (Figure 2B, inset). We can identify ILVs in these images (arrows). In fact, 12% of 535 2D images show evidence for at least one and up to three ILV's per granule. To clearly identify the internal vesicles in the context of granule architecture without the ambiguity of overlap in the 2D image, we performed electron cryotomography and volume reconstruction. Figure 3 (and Supplementary video S4) shows a tomogram section containing WPBs, other vesicular organelles, cytoskeletal filaments, ribosomes, and other particles. ILVs within WPBs are indicated by arrows. The lumen of WPB ILVs was less electron dense than the surrounding VWF tubules, being similar in density to the lumen of ILVs of MVBs and to regions of cell cytosol.

We built structural models for 22 ILVs from 15 tomograms (Figures 4, 5 and Supplementary Figure S3). ILVs were not confined to regions close to the ends of WPBs, but could be seen at any point up to mid-body. In many cases the membrane of the ILV was in close apposition to the WPB limiting membrane and sometimes associated with a bulge in the WPB limiting membrane. ILVs were often non-spherical in shape, appearing compressed between the smooth limiting membrane of the WPB and VWF tubules. As previously observed WPBs contained paracrystals of helical VWF, shown in cross section as indicated in Figure 4A and Supplementary video S5. A prominent membrane-bounded ILV can be seen where the paracrystalline packing is disrupted giving the granule a club-shape, a common morphology for WPBs. WPB ILVs were also observed in adult human heart microvascular endothelial cells (HHMEC) (Figure 4B and Supplementary Figure S3C) confirming that these structures are not specific to HUVEC but represent a general feature of endothelial WPBs.

We observed many WPB ILVs of HUVEC or HHMEC to contain densities and structures resembling cytoplasmic components (Figure 4 B,C and Supplementary Figure S4 and video S6). Measurements of WPB ILVs and ILVs of single- and multi-vesicular bodies (MVBs) and single internal vesicle bodies in tomograms (Figure 5) showed them to have a similar size distribution and include some large outliers (e.g. ILV in WPB in Supplementary Figure S3A). The majority of ILVs in WPBs (mean volume 147,292±41,225 nm^3, sem, n=15 measurements) are similar in size to the small vesicles within the MVBs (mean volume 165,286±30,664 nm^3, sem, n=25) (see Supplementary video S7).

WPB ILVs contain CD63 derived from the endocytic pathway but may differ in composition from ILVs in MVBs

Because endogenous CD63 cycles from the plasma membrane to WPBs via the endocytic pathway [7,9,10] we next examined whether CD63 in WPB ILVs was also derived from this trafficking route by monitoring the accumulation of an extracellularly applied TRITC-labelled mouse anti-human CD63 antibody in WPBs as previously described [7] (Figure 6). The TRITC-anti-CD63 antibody (but not a

non-targeting mouse IgG_1 control antibody, Supplementary Figure S5) was readily trafficked to WPBs (Figure 6A) and in both control and EGFP-CD63-expressing HUVEC was enriched within WPB ILVs (Figure 6B-C) confirming that WPB ILV CD63 is of endosomal origin. We next looked for evidence in WPB-ILVs of other components reported to be present in ILVs of endosomal origin. Biochemical studies have identified cholesterol as one of the lipids enriched in exosomes [34]. Localization of cholesterol-rich regions by filipin staining in HUVEC, showed abundant labelling of endosomal/lysosomal structures but no labelling of WPBs (Supplementary Figure S6C). Some [35] but not all [36] studies suggest that LE/MVBs and their ILVs are enriched in lysobisphosphatidic acid (LBPA). Immuno-staining of HUVEC for endogenous LBPA, showed a striking punctate enrichment within LE/MVBs but no labelling of WPBs (Supplementary Figure S6Ai), a result consistent with a previous study [9]. The fluorescent phosphatidyl ethanolamine (PE) analogue, N-Rh-PE (1,2-dipalmitoyl-sn-glycero-3-phosphoethanolamine-N-[lissamine rhodamine B sulfonyl]), is taken up from the plasma membrane, trafficked to LE\MVBs and incorporated into exosomes [37,38]. Incubation of HUVEC with N-Rh-PE revealed no WPB staining (Supplementary Figure S6Bi-ii). Other common exosomal markers, including CD9, CD81, along with several ESCRT components including Alix, TSG101, VSP2/Chmp2B, HSP70 and the autophagy marker LC3 were not detected in WPBs (Supplementary Figures S7 and S8). However, we did detect the PDZ domain containing adapter protein, syntenin, associated with WPBs (Supplementary Figure S8B). Together the results suggest WPB ILVs have a distinct composition.

Direct observation of ILV secretion during WPB exocytosis

Having established that WPBs do contain ILVs we next asked whether these could be released during exocytosis. If so, we predicted that WPB associated EGFP-CD63 microdomains (ILVs) would be released as discrete fluorescent particles during WPB exocytosis. To test this we monitored histamine-evoked WPB exocytosis in live HUVEC co-expressing VWF-mCherry and EGFP-CD63 using high-speed epifluorescence imaging. EGFP-CD63 labeled ILVs were released as discrete

particles from individual WPBs during histamine stimulation (Figure 7). Panels A-D show image sequences taken from Supplementary videos S8, S9, S10 and S11 respectively. In examples A-C the EGFP-CD63 particles (arrows) escape rapidly into the bulk solution and are lost from view. D shows an example of the particle becoming trapped within the extracellular patch of VWF secreted during WPB exocytosis. In addition to direct release into the bulk solution the particles were also secreted into the narrow two-dimensional plane between the cell and the glass coverslip. In these cases the extracellular diffusion of the particles could be visualized for long periods before the particles eventually encountered the cell edge and escaped into the bulk media (e.g. Supplementary video S12). Consistent with our ultrastructural data, we also observed release of multiple ILVs from single WPB (Supplementary video S13). Thus CD63-containing ILVs are released from the interior of the WPB to the extracellular medium along with VWF during exocytosis.

Discussion

Here we demonstrate that WPBs contain CD63-postive ILVs and release them during secretagogue-evoked exocytosis. Shedding of plasma membrane-derived vesicles and MVB-plasma membrane fusion has been visualized in live cells [21,39,40], however, direct imaging of ILV release from individual regulated secretory granules during exocytosis has not been reported previously. To indicate their specific origin, we refer to the secreted vesicles described here as WPB-released exosomes.

Our cryomicroscopy studies of the thin periphery of endothelial cells show that mature WPBs contain ILV's that are either embedded within and distort the paracrystalline assemblies of VWF tubules or are squeezed between the VWF paracrystal and the tightly wrapped granule-limiting membrane. This accounts for their immobility within the granule.

During exocytosis WPB-released exosomes are secreted into the surrounding medium, although they may initially be entangled by the secreted VWF. In other systems, tethering has been proposed as a mechanism of restricting exosomes to local target sites [41]. WPB exocytic events involve complex structural changes in the granule [1] and may selectively release small molecules to the bloodstream as well as CD63 to the plasma membrane without releasing VWF [42]. ILV release adds an additional signaling diversity to these exocytic events.

The identification of CD63-rich ILV's within the WPB lumen extends the features that WPBs share with other LROs. Many LROs, such as melanosomes and lytic granules, release CD63-rich vesicles. Our observations draw further attention to the similarity of WPBs to platelet α-granules which originate as MVBs containing ILVs, but during maturation become filled with dense material, including VWF and P-selectin. In addition, our immunofluorescence data show that WPB ILVs are enriched in CD63 but lack CD9 or CD81, which is also the case with the ILVs of platelet α-granules [18].

In contrast to platelet α-granules, WPBs form by the polymerization of VWF in nascent granules at the TGN. Protrusive clathrin-coated membrane buds are a feature of nascent WPBs, reflecting the active sorting away of material not destined for storage in the mature WPB [43]. Mature WPBs lack bilayer coats [3,43,44] and our cryo-EM images of vitrified endothelial cells show a tight, almost shrink wrapped limiting membrane surrounding the paracrystalline core of VWF and associated ILVs.

Newly forming WPBs emerging from the TGN lack CD63, but soon after acquire the tertraspannin through a poorly defined interaction with endosomal components [9,10] that involve the adapter protein AP3 and Annexin 8 [7,10]. These observations (on WPBs and platelet α-granules) contribute to a view in which the LRO possesses a mixture of endosomal vs regulated secretory features that depend on the organelle's biogenesis and specialisation.

In this study we have shown that the CD63 in WPB ILVs is trafficked via the endosomal system. CD63 is a ubiquitously expressed integral membrane protein found on the plasma membrane and endosomal compartments of all cells [45]. In endosomal compartments CD63 is enriched in a subset of ILVs and is present on exosomes secreted during MVB fusion with the plasma membrane [34,46,47]. CD63 delivery to WPBs could occur through small vesicles formed by endosomal membrane budding [48]. Such vesicles can contain AP3 [49], the adapter protein implicated in CD63 delivery to WPBs [10]. Alternatively, direct fusion and content transfer between LE\MVBs and lysosomal compartments is well documented [50] and a similar process could account for diffusional transfer of CD63 to the limiting membrane of the maturing WPB, as well as direct MVB to WPB ILV transfer. The absence in WPBs of several markers reported to be enriched in ILVs/exosomes of LE/MVBs; Lysobisphosphatidic acid (LPBA) [9], cholesterol [36], CD9 and CD81 [32,45], as well as exogenous markers reported to accumulate in LE/MVB ILVs; N-Rh-PE [37], indicate that WPB ILVs may represent a distinct population with similarities to those of platelet α-granules.

We looked for the presence of ESCRT components and associated proteins known to be involved in

MVB exosome formation and found syntenin localized to WPBs. Syntenin is a cytosolic PDZ domain protein that acts as an intracellular adapter involved in many processes including exosome biogenesis and secretion [51]. Syntenin binds directly to CD63 [52] and regulates formation of CD63-containing exosomes [51,53]. The localization of CD63 and syntenin on WPBs, the presence of cytoplasmic components within WPB ILVs may indicate formation of WPB ILVs by inward budding of the WPB limiting membrane during organelle maturation.

Growing evidence suggests that endothelial derived exosomes provide an important route for the exchange of proteins, lipids and nucleic acids that contribute to intercellular communication and regulation of the immune and cardiovascular systems [54,55]. Endothelial cell derived exosomes are reported to directly modulate many different target cells, [47,56,57], and in turn endothelial cells are a target for exosomes released from other cells [58-61]. For example, angiopoietin-2 (Ang2), an important regulator of vascular network formation, is secreted from endothelial cells on the outer surface of CD63-positive exosomes [47]. While the etiology of these secreted exosomes has been assumed to be LE/MVBs, Ang2 can be stored in the lumen of WPBs for regulated secretion [62], raising the intriguing possibility that some of these vesicles may be released through WPB exocytosis.

Endothelial cells accumulate hundreds of WPBs under resting conditions and may contain similar numbers of MVBs [1,21]. During Ca^{2+}-stimulation WPB exocytosis is rapid in onset, peaking 5-10 seconds after stimulation, involves up to 50% of the stored organelles and is largely complete within 1-2 minutes of stimulation [63]. Ca^{2+}-stimulated MVB fusion is reported to be slower in onset (2-6 minutes), involves a subpopulation of CD63+ MVBs [21,40,64] and is estimated to result in only a small fraction (~3%) of CD63+ MVB ILVs being released as exosomes [21]. WPBs are therefore well placed for exosome release following acute cell activation and prior to exosome release by MVB-fusion.

Addendum

J.S. A-V.F,J.T., N.I.K.,L.K.,T.C performed research and analyzed data; P.R. and T.C. designed the research; and wrote the paper. The authors report no disclosures.

Acknowledgements

The anti-CD63 monoclonal antibody H5C6 developed by August, J.T. and Hildreth, J.E.K. was obtained from the Developmental Studies Hybridoma Bank, created by the NICHD of the NIH and maintained at The University of Iowa, Department of Biology, Iowa City, IA 52242. TC was funded by the UK Medical Research Council under program grants MC_PC_13053. P.B.R. is supported by the Francis Crick Institute, which receives its core funding from Cancer Research UK (FC001156 and FC001143), the UK Medical Research Council (FC001156 and FC001143), and the Wellcome Trust (FC001156 and FC001143).

References

1. Schillemans M, Karampini E, Kat M, Bierings R. Exocytosis of Weibel-Palade bodies: how to unpack a vascular emergency kit. *J Thromb Haemost*. 2018;17(1):6-18.
2. Tkach M, Thery C. Communication by Extracellular Vesicles: Where We Are and Where We Need to Go. *Cell*. 2016;164(6):1226-1232.
3. Berriman JA, Li S, Hewlett LJ, et al. Structural organization of Weibel-Palade bodies revealed by cryo-EM of vitrified endothelial cells. *Proc Natl Acad Sci U S A*. 2009;106(41):17407-17412.
4. Sadler JE. von Willebrand factor assembly and secretion. *J Thromb Haemost*. 2009;7 Suppl 1:24-27.
5. Zhou YF, Eng ET, Nishida N, Lu C, Walz T, Springer TA. A pH-regulated dimeric bouquet in the structure of von Willebrand factor. *EMBO J*. 2011;30(19):4098-4111.
6. Doyle EL, Ridger V, Ferraro F, Turmaine M, Saftig P, Cutler DF. CD63 is an essential cofactor to leukocyte recruitment by endothelial P-selectin. *Blood*. 2011;118(15):4265-4273.
7. Poeter M, Brandherm I, Rossaint J, et al. Annexin A8 controls leukocyte recruitment to activated endothelial cells via cell surface delivery of CD63. *Nat Commun*. 2014;5:3738-.
8. Toothill VJ, Van Mourik JA, Niewenhuis HK, Metzelaar MJ, Pearson JD. Characterization of the enhanced adhesion of neutrophil leukocytes to thrombin-stimulated endothelial cells. *J Immunol*. 1990;145(1):283-291.
9. Kobayashi T, Vischer UM, Rosnoblet C, et al. The tetraspanin CD63/lamp3 cycles between endocytic and secretory compartments in human endothelial cells. *Mol Biol Cell*. 2000;11(5):1829-1843.
10. Harrison-Lavoie KJ, Michaux G, Hewlett L, et al. P-selectin and CD63 use different mechanisms for delivery to Weibel-Palade bodies. *Traffic*. 2006;7(6):647-662.
11. Marks MS, Heijnen HF, Raposo G. Lysosome-related organelles: unusual compartments become mainstream. *Curr Opin Cell Biol*. 2013;25(4):495-505.
12. Raposo G, Nijman HW, Stoorvogel W, et al. B lymphocytes secrete antigen-presenting vesicles. *J Exp Med*. 1996;183(3):1161-1172.
13. Raposo G, Marks MS, Cutler DF. Lysosome-related organelles: driving post-Golgi compartments into specialisation. *Curr Opin Cell Biol*. 2007;19(4):394-401.
14. Zografou S, Basagiannis D, Papafotika A, et al. A complete Rab screening reveals novel insights in Weibel-Palade body exocytosis. *J Cell Sci*. 2012;125(Pt 20):4780-4790.
15. Bierings R, Hellen N, Kiskin N, et al. The interplay between the Rab27A effectors Slp4-a and MyRIP controls hormone-evoked Weibel-Palade body exocytosis. *Blood*. 2012;120(13):2757-2767.
16. Nightingale TD, Pattni K, Hume AN, Seabra MC, Cutler DF. Rab27a and MyRIP regulate the amount and multimeric state of VWF released from endothelial cells. *Blood*. 2009;113(20):5010-5018.
17. van Breevoort D, Snijders AP, Hellen N, et al. STXBP1 promotes Weibel-Palade body exocytosis through its interaction with the Rab27A effector Slp4-a. *Blood*. 2014;123(20):3185-3194.
18. Heijnen HF, Schiel AE, Fijnheer R, Geuze HJ, Sixma JJ. Activated platelets release two types of membrane vesicles: microvesicles by surface shedding and exosomes derived from exocytosis of multivesicular bodies and alpha-granules. *Blood*. 1999;94(11):3791-3799.
19. Blanchard N, Lankar D, Faure F, et al. TCR activation of human T cells induces the production of exosomes bearing the TCR/CD3/zeta complex. *J Immunol*. 2002;168(7):3235-3241.
20. Ostrowski M, Carmo NB, Krumeich S, et al. Rab27a and Rab27b control different steps of the exosome secretion pathway. *Nat Cell Biol*. 2010;12(1):19-30; sup pp 11-13.
21. Messenger SW, Woo SS, Sun Z, Martin TFJ. A Ca(2+)-stimulated exosome release pathway in cancer cells is regulated by Munc13-4. *J Cell Biol*. 2018;217(8):2877-2890.
22. Meli A, Carter T, McCormack A, Hannah MJ, Rose ML. Antibody alone is not a stimulator of exocytosis of Weibel-Palade bodies from human endothelial cells. *Transplantation*. 2012;94(8):794-801.
23. Hewlett L, Zupancic G, Mashanov G, et al. Temperature-dependence of Weibel-Palade body exocytosis and cell surface dispersal of von Willebrand factor and its propolypeptide. *PLoS One*. 2011;6(11):e27314.
24. Mastronarde DN. Dual-axis tomography: an approach with alignment methods that preserve resolution. *J Struct Biol*. 1997;120(3):343-352.
25. Kiskin NI, Hellen N, Babich V, et al. Protein mobilities and P-selectin storage in Weibel-Palade bodies. *J Cell Sci*. 2010;123(Pt 17):2964-2975.
26. Kiskin NI, Babich V, Knipe L, Hannah MJ, Carter T. Differential cargo mobilisation within Weibel-Palade bodies after transient fusion with the plasma membrane. *PLoS One*. 2014;9(9):e108093.
27. Kowal J, Arras G, Colombo M, et al. Proteomic comparison defines novel markers to characterize heterogeneous populations of extracellular vesicle subtypes. *Proc Natl Acad Sci U S A*. 2016;113(8):E968-977.
28. Bobrie A, Colombo M, Krumeich S, Raposo G, Thery C. Diverse subpopulations of vesicles secreted by different intracellular mechanisms are present in exosome preparations obtained by differential ultracentrifugation. *J Extracell Vesicles*. 2012;1.
29. van Niel G, Charrin S, Simoes S, et al. The tetraspanin CD63 regulates ESCRT-independent and -dependent endosomal sorting during melanogenesis. *Dev Cell*. 2011;21(4):708-721.
30. Suetsugu A, Honma K, Saji S, Moriwaki H, Ochiya T, Hoffman RM. Imaging exosome transfer from breast

cancer cells to stroma at metastatic sites in orthotopic nude-mouse models. *Adv Drug Deliv Rev*. 2013;65(3):383-390.
31. Vischer UM, Wagner DD. CD63 is a component of Weibel-Palade bodies of human endothelial cells. *Blood*. 1993;82(4):1184-1191.
32. Escola JM, Kleijmeer MJ, Stoorvogel W, Griffith JM, Yoshie O, Geuze HJ. Selective enrichment of tetraspan proteins on the internal vesicles of multivesicular endosomes and on exosomes secreted by human B-lymphocytes. *J Biol Chem*. 1998;273(32):20121-20127.
33. Espenel C, Margeat E, Dosset P, et al. Single-molecule analysis of CD9 dynamics and partitioning reveals multiple modes of interaction in the tetraspanin web. *J Cell Biol*. 2008;182(4):765-776.
34. Colombo M, Raposo G, Thery C. Biogenesis, secretion, and intercellular interactions of exosomes and other extracellular vesicles. *Annu Rev Cell Dev Biol*. 2014;30:255-289.
35. Kobayashi T, Stang E, Fang KS, de Moerloose P, Parton RG, Gruenberg J. A lipid associated with the antiphospholipid syndrome regulates endosome structure and function. *Nature*. 1998;392(6672):193-197.
36. Wubbolts R, Leckie RS, Veenhuizen PT, et al. Proteomic and biochemical analyses of human B cell-derived exosomes. Potential implications for their function and multivesicular body formation. *J Biol Chem*. 2003;278(13):10963-10972.
37. Vidal M, Mangeat P, Hoekstra D. Aggregation reroutes molecules from a recycling to a vesicle-mediated secretion pathway during reticulocyte maturation. *J Cell Sci*. 1997;110 (Pt 16):1867-1877.
38. Willem J, ter Beest M, Scherphof G, Hoekstra D. A non-exchangeable fluorescent phospholipid analog as a membrane traffic marker of the endocytic pathway. *Eur J Cell Biol*. 1990;53(1):173-184.
39. MacKenzie A, Wilson HL, Kiss-Toth E, Dower SK, North RA, Surprenant A. Rapid secretion of interleukin-1beta by microvesicle shedding. *Immunity*. 2001;15(5):825-835.
40. Verweij FJ, Bebelman MP, Jimenez CR, et al. Quantifying exosome secretion from single cells reveals a modulatory role for GPCR signaling. *J Cell Biol*. 2018;217(3):1129-1142.
41. Edgar JR, Manna PT, Nishimura S, Banting G, Robinson MS. Tetherin is an exosomal tether. *Elife*. 2016;5.
42. Babich V, Meli A, Knipe L, et al. Selective release of molecules from Weibel-Palade bodies during a lingering kiss. *Blood*. 2008;111(11):5282-5290.
43. Zenner HL, Collinson LM, Michaux G, Cutler DF. High-pressure freezing provides insights into Weibel-Palade body biogenesis. *J Cell Sci*. 2007;120(Pt 12):2117-2125.
44. Valentijn KM, van Driel LF, Mourik MJ, et al. Multigranular exocytosis of Weibel-Palade bodies in vascular endothelial cells. *Blood*. 2010;116(10):1807-1816.
45. Pols MS, Klumperman J. Trafficking and function of the tetraspanin CD63. *Exp Cell Res*. 2009;315(9):1584-1592.
46. Kowal J, Tkach M, Thery C. Biogenesis and secretion of exosomes. *Curr Opin Cell Biol*. 2014;29:116-125.
47. Ju R, Zhuang ZW, Zhang J, et al. Angiopoietin-2 secretion by endothelial cell exosomes: regulation by the phosphatidylinositol 3-kinase (PI3K)/Akt/endothelial nitric oxide synthase (eNOS) and syndecan-4/syntenin pathways. *J Biol Chem*. 2014;289(1):510-519.
48. Theos AC, Tenza D, Martina JA, et al. Functions of adaptor protein (AP)-3 and AP-1 in tyrosinase sorting from endosomes to melanosomes. *Mol Biol Cell*. 2005;16(11):5356-5372.
49. Peden AA, Oorschot V, Hesser BA, Austin CD, Scheller RH, Klumperman J. Localization of the AP-3 adaptor complex defines a novel endosomal exit site for lysosomal membrane proteins. *J Cell Biol*. 2004;164(7):1065-1076.
50. Luzio JP, Pryor PR, Bright NA. Lysosomes: fusion and function. *Nat Rev Mol Cell Biol*. 2007;8(8):622-632.
51. Baietti MF, Zhang Z, Mortier E, et al. Syndecan-syntenin-ALIX regulates the biogenesis of exosomes. *Nat Cell Biol*. 2012;14(7):677-685.
52. Latysheva N, Muratov G, Rajesh S, et al. Syntenin-1 is a new component of tetraspanin-enriched microdomains: mechanisms and consequences of the interaction of syntenin-1 with CD63. *Mol Cell Biol*. 2006;26(20):7707-7718.
53. Friand V, David G, Zimmermann P. Syntenin and syndecan in the biogenesis of exosomes. *Biol Cell*. 2015;107(10):331-341.
54. Dignat-George F, Boulanger CM. The many faces of endothelial microparticles. *Arterioscler Thromb Vasc Biol*. 2011;31(1):27-33.
55. Sluijter JP, Verhage V, Deddens JC, van den Akker F, Doevendans PA. Microvesicles and exosomes for intracardiac communication. *Cardiovasc Res*. 2014;102(2):302-311.
56. Sheldon H, Heikamp E, Turley H, et al. New mechanism for Notch signaling to endothelium at a distance by Delta-like 4 incorporation into exosomes. *Blood*. 2010;116(13):2385-2394.
57. Hergenreider E, Heydt S, Treguer K, et al. Atheroprotective communication between endothelial cells and smooth muscle cells through miRNAs. *Nat Cell Biol*. 2012;14(3):249-256.
58. Al-Nedawi K, Szemraj J, Cierniewski CS. Mast cell-derived exosomes activate endothelial cells to secrete plasminogen activator inhibitor type 1. *Arterioscler Thromb Vasc Biol*. 2005;25(8):1744-1749.
59. Umezu T, Ohyashiki K, Kuroda M, Ohyashiki JH. Leukemia cell to endothelial cell communication via exosomal miRNAs. *Oncogene*. 2013;32(22):2747-2755.
60. Gambim MH, do Carmo Ade O, Marti L, Verissimo-Filho S, Lopes LR, Janiszewski M. Platelet-derived exosomes induce endothelial cell apoptosis through peroxynitrite generation: experimental evidence for a novel mechanism of septic vascular dysfunction. *Crit Care*. 2007;11(5):R107.

61. Lee HD, Kim YH, Kim DS. Exosomes derived from human macrophages suppress endothelial cell migration by controlling integrin trafficking. *Eur J Immunol*. 2014;44(4):1156-1169.
62. Fiedler U, Scharpfenecker M, Koidl S, et al. The Tie-2 ligand angiopoietin-2 is stored in and rapidly released upon stimulation from endothelial cell Weibel-Palade bodies. *Blood*. 2004;103(11):4150-4156.
63. Erent M, Meli A, Moisoi N, et al. Rate, extent and concentration dependence of histamine-evoked Weibel-Palade body exocytosis determined from individual fusion events in human endothelial cells. *J Physiol*. 2007;583(Pt 1):195-212.
64. Savina A, Furlan M, Vidal M, Colombo MI. Exosome release is regulated by a calcium-dependent mechanism in K562 cells. *J Biol Chem*. 2003;278(22):20083-20090.

Figures

Figure 1

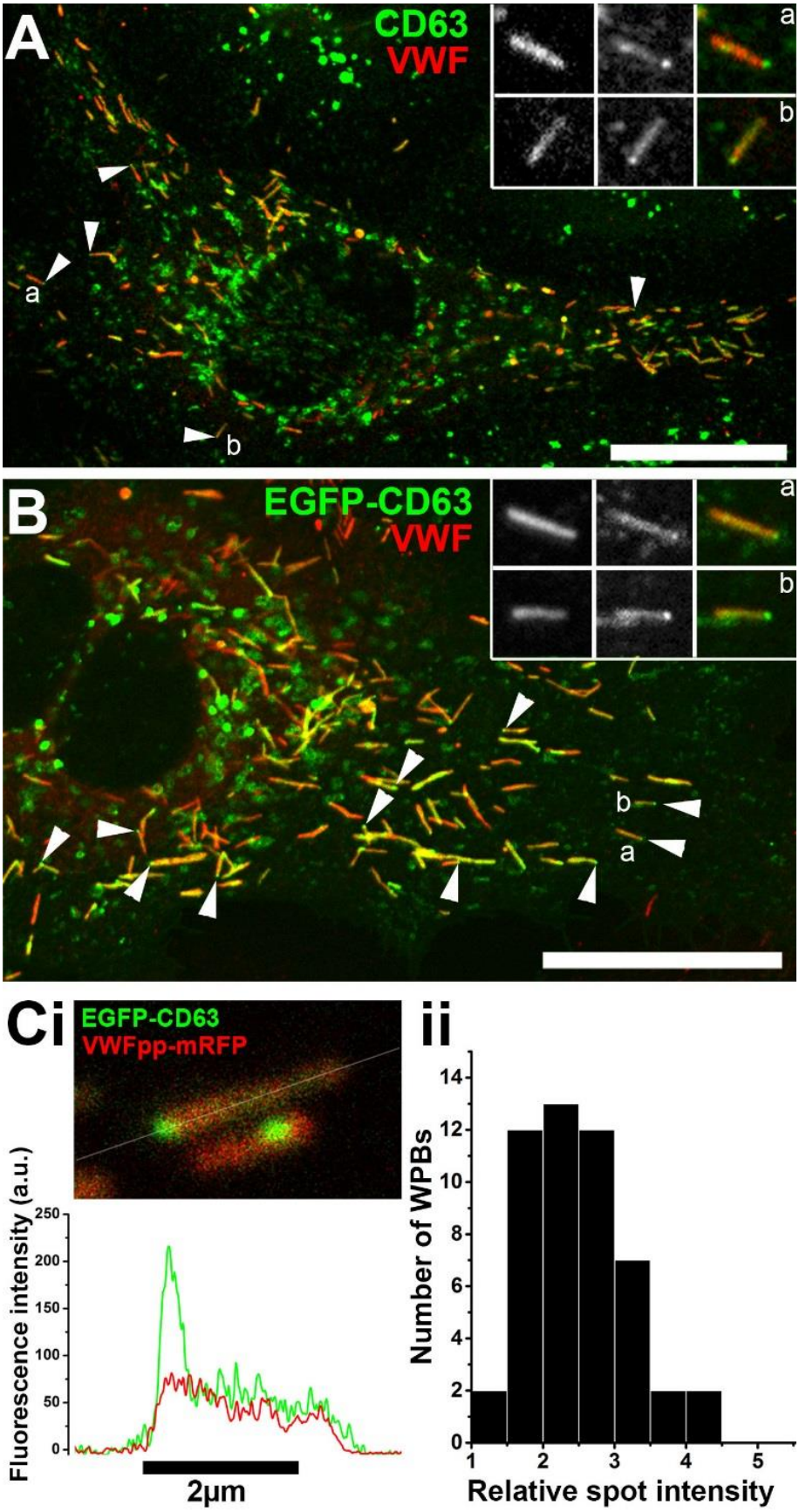

Figure 1. CD63 is enriched in micro domains on WPBs.

A-B; Confocal images of single fixed HUVEC (A) immuno-labelled with specific antibodies to CD63 (green) and VWF (red) or (B) expressing exogenous EGFP-CD63 (green) and immuno-labelled for VWF (red). Scale bars are 10µm. Arrow heads indicate bright regions of CD63 (A) or EGFP-CD63 (B) closely associated with individual WPBs. Inset panels show on expanded scales the fluorescence, in grey scale, for VWF (left) and CD63 (middle) and the colour merge image (right; VWF in red, CD63 in green) for WPBs indicated by a and b. Images A and B were taken at room temperature using a Leica SP2 confocal microscope and software (Mannheim, Germany) equipped with a PL APO100x 1.4NA objective. (Ci) Image from a live cell confocal fluorescence experiment of an EGFP-CD63 (green) and VWFpp-mRFP (red) co-expressing HUVEC showing two WPBs containing discrete bright micro-domains of EGFP-CD63 fluorescence. Intensity plots through the long axis of the upper WPB (white line) are shown below (green: CD63, red VWFpp). (Cii) Histogram of the fold increase in mean EGFP fluorescence intensity in micro-domains compared to non-micro-domain regions (bulk WPB membrane) for 50 WPBs. Mean micro-domain EGFP intensity was 2.5±0.7 fold (n=49 WPbs, range 1.4-4.1) that in the bulk membrane of the corresponding WPB. Images in C were taken at 37°C using a Leica SP5 with a HCX PL APO CS 100.0x 1.46NA Oil objective, pinhole (airy) 1.5, zoom 30-35.5, scan speed 1400Hz in xyt acquisition mode.

Figure 2

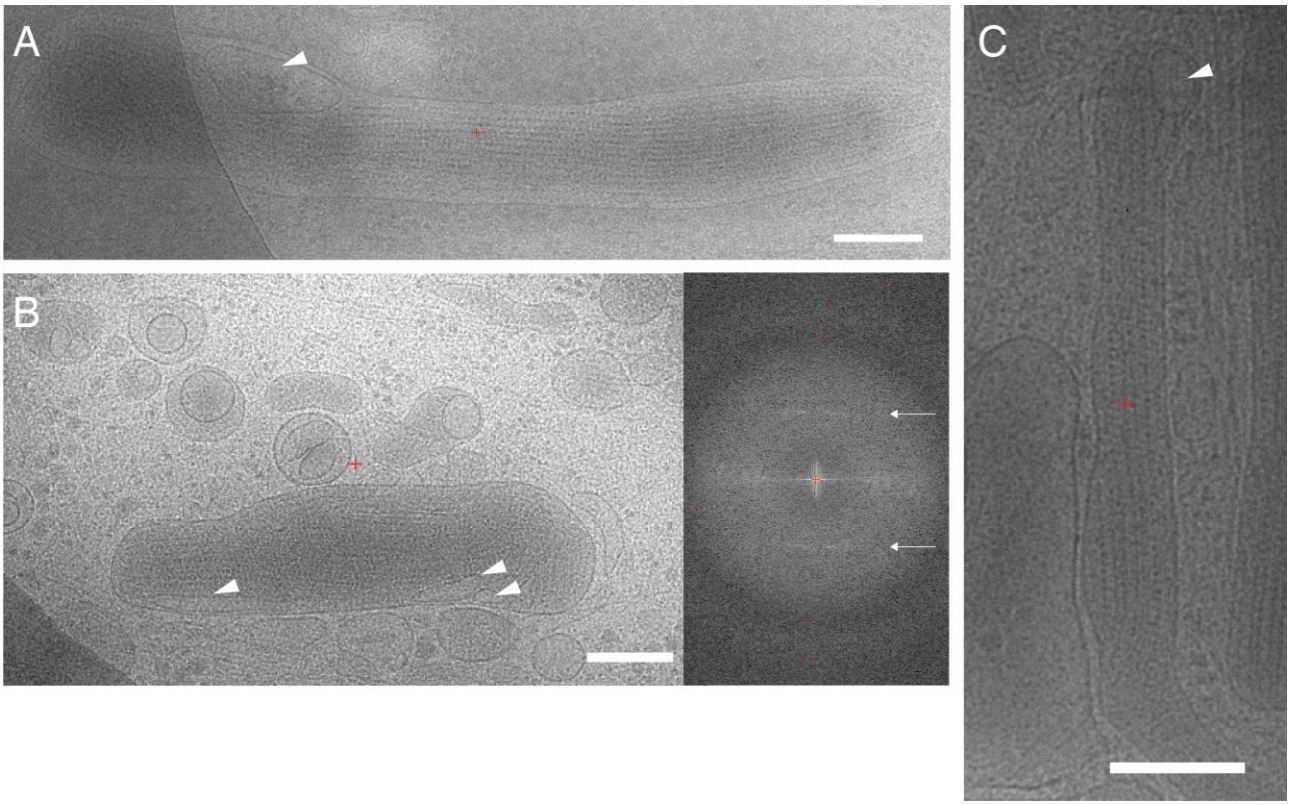

Figure 2. Electron cryomicroscopy of frozen-hydrated HUVECs showing Weibel-Palade Bodies in cytoplasm.

A-C 2D images of Weibel-Palade Bodies show internal density for VWF tubules. ILVs are indicated by triangular white arrows. Fourier transform of WPB interior in B shows helical layer lines for VWF (arrows). Scale bars are 200 nm.

Figure 3

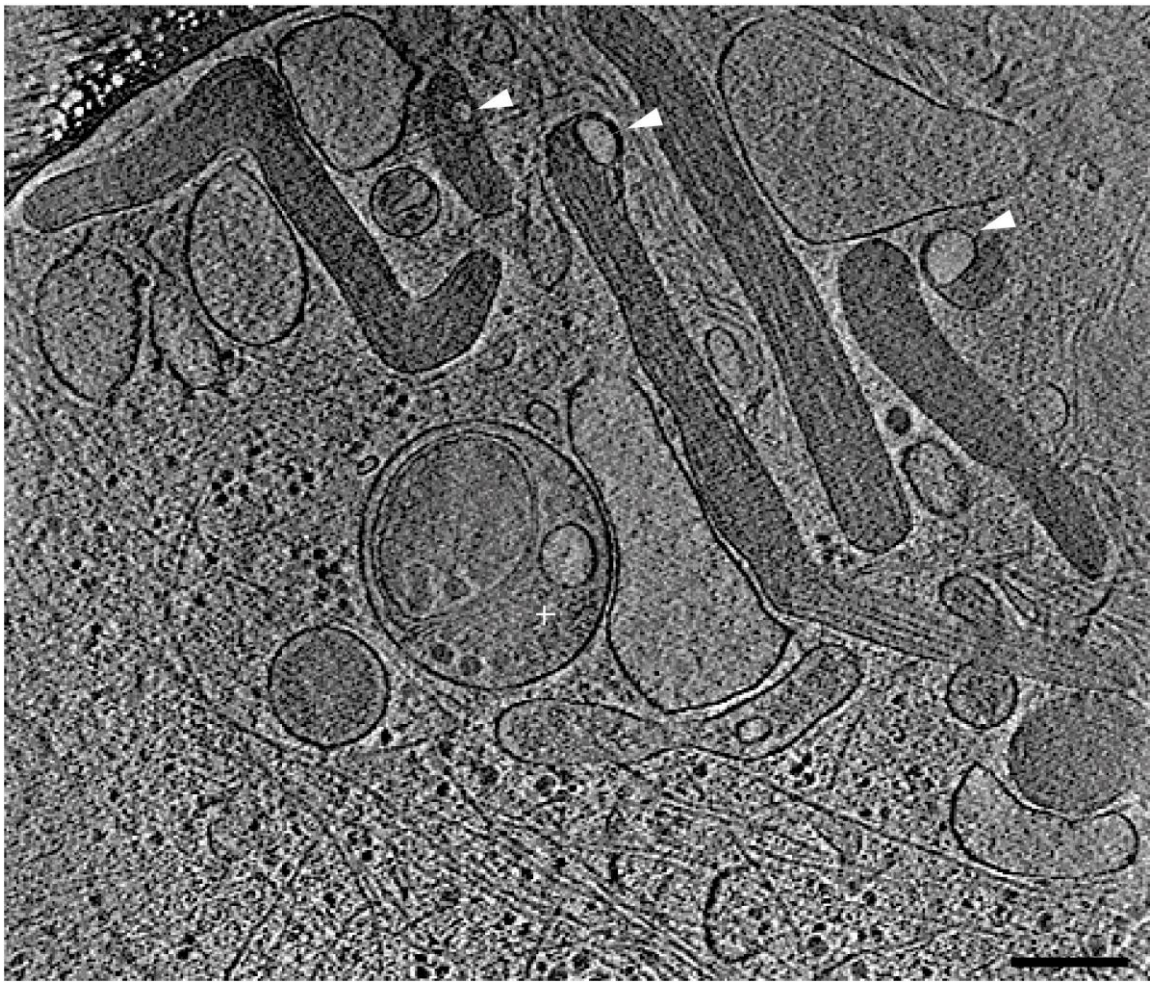

Figure 3. Section of an electron cryotomogram of a frozen-hydrated endothelial cell showing region with Weibel-Plade bodies. ILV's within Weibel-Palade bodies indicated by arrow. Scale bar is 200 nm.

Figure 4

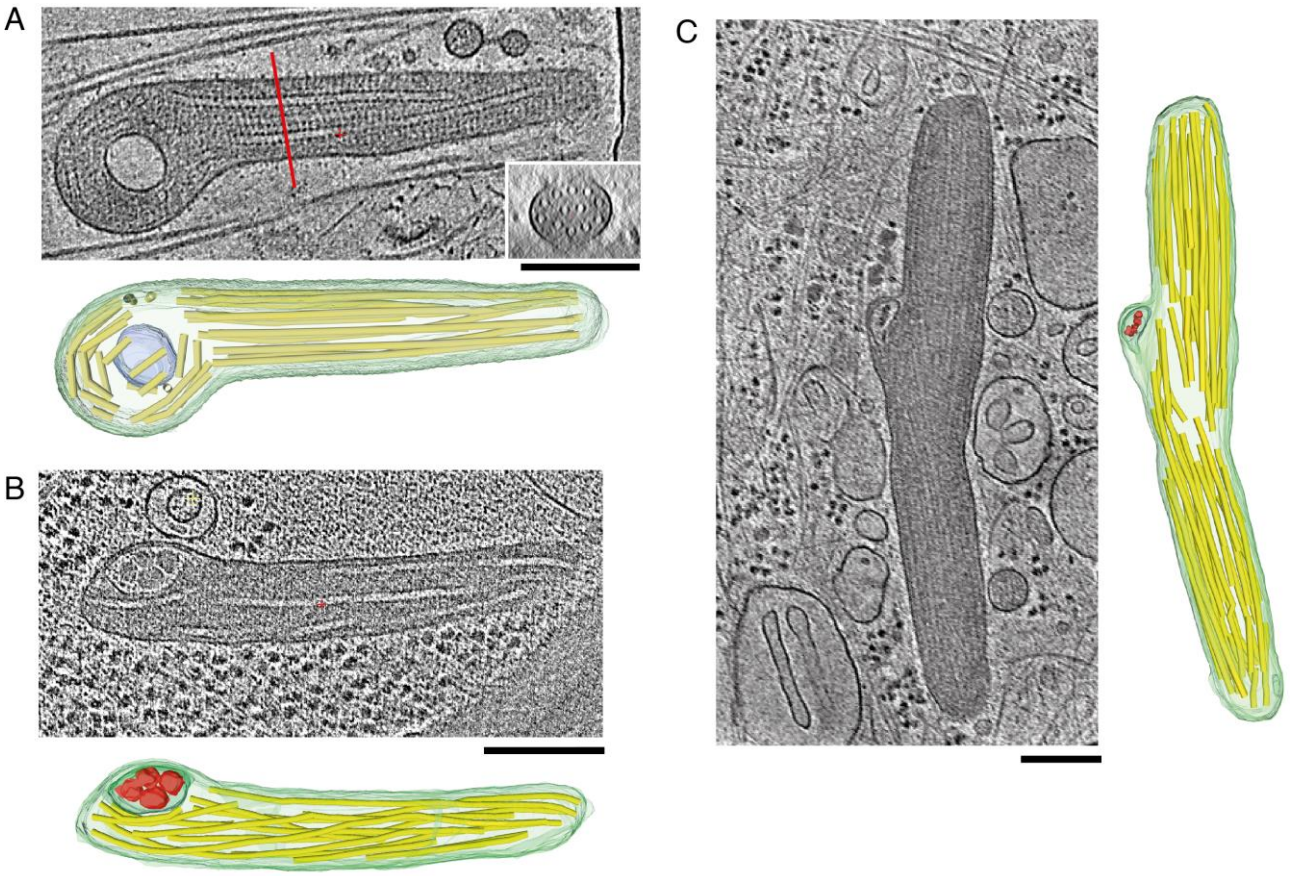

Figure. 4. Tomogram sections of Weibel-Palade bodies containing ILVs along with structural models.

Tomogram section with structural model consisting of WPB limiting model green, ILV membrane blue-green, VWF tubules yellow, and ILV internal content, red. (A) inset shows tomogram cross-section at location of red line. (B) WPB from an HHMEC with an ILV at the left side of the granule. The ILV contains internal content similar to cytoplasmic granules as shown in Supplementary Figure S4. (C) WPB in a HUVEC with kink in the middle where tubules have disrupted the paracrystalline order. The ILV contains density similar in size to cytosolic densities visible throughout tomogram section. Scale bars are 200 nm.

Figure 5

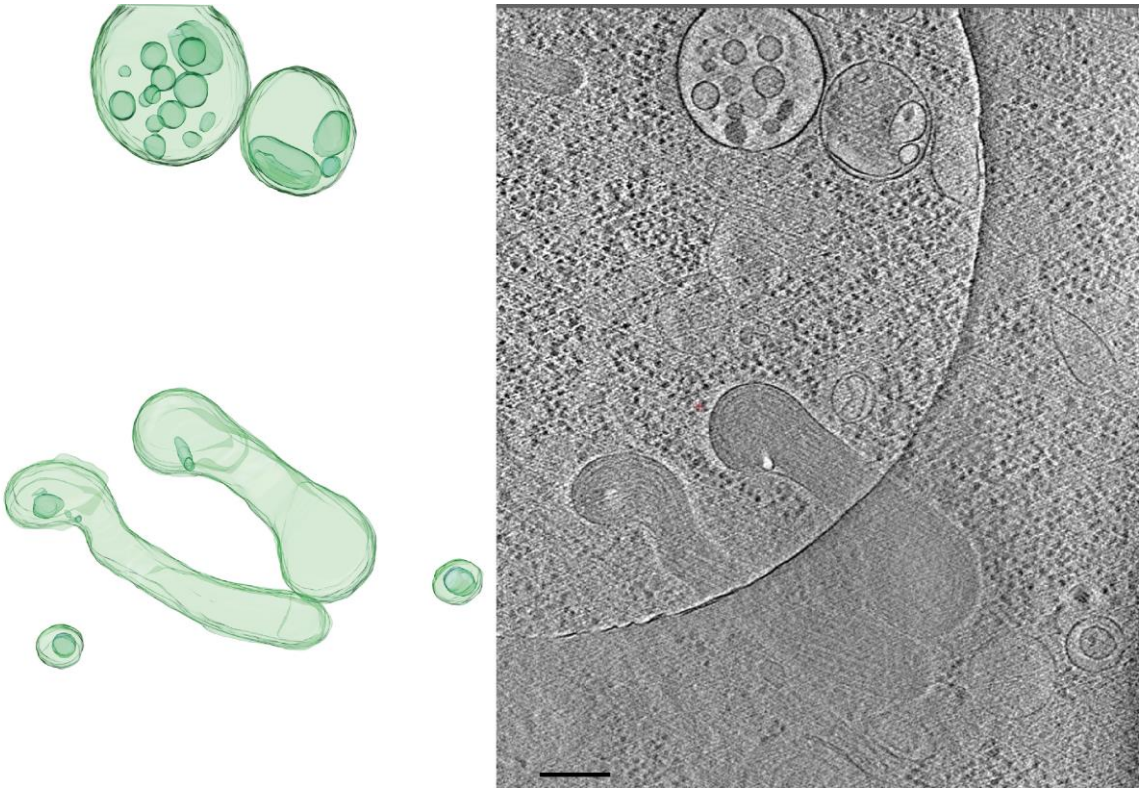

Figure 5. Tomogram section showing WPBs and MVBs.

Tomogram section (right) shows WPBs and MVBs containing ILVs as indicated in structural model (left).

Figure 6

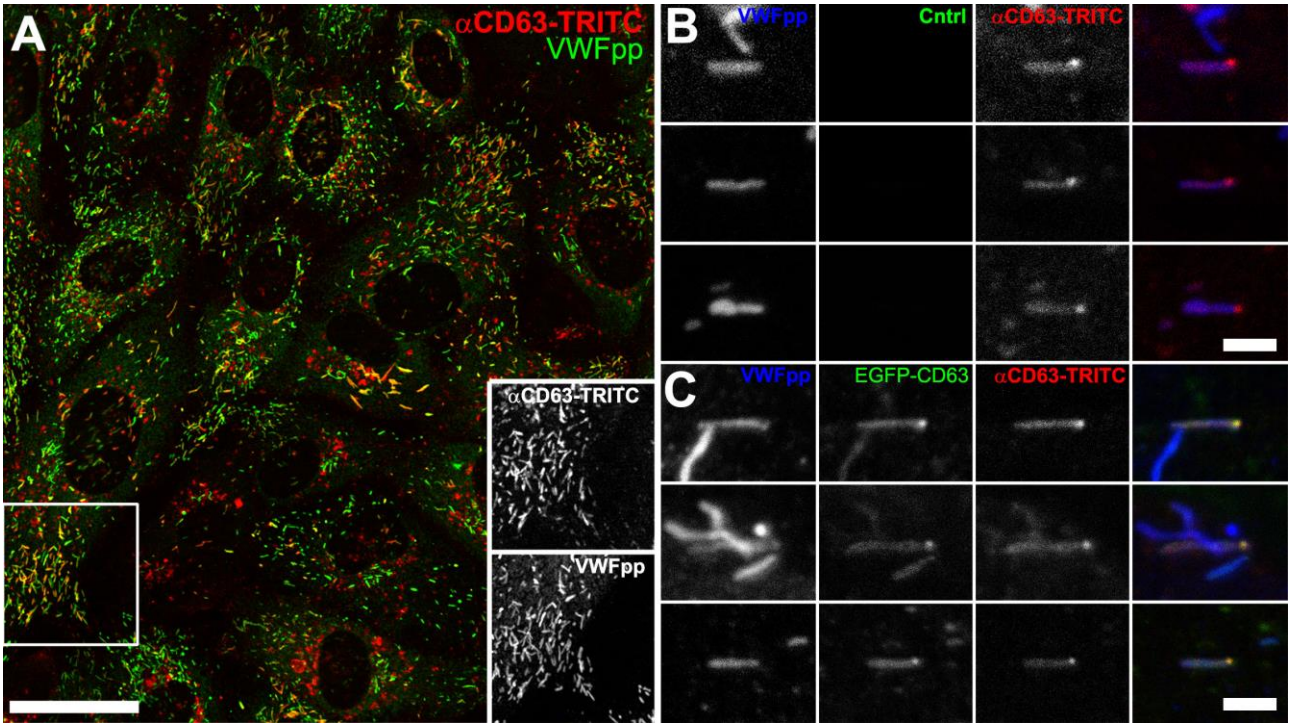

Figure 6 CD63 in WPB ILVs is of endosomal origin. (A) confocal fluorescence image of HUVEC incubated live in the presence of an extracellular TRITC-conjugated mouse anti-CD63 antibody (red; 1:55 dilution, 24 h). The cells were fixed and immunolabelled with a specific antibody to VWFpp (green). Scale bar 20µm. The region indicated by the white box is shown as grey scale inserts to illustrate the accumulation of extracellular applied TRITC-anti-CD63 in WPBs. (B-C) examples of the accumulation of extracellular applied TRITC-anti-CD63 in micro-domains in WPBs in control (B; mock transfected) or EGFP-CD63 transfected (C) HUVEC incubated live with the TRITC-anti-CD63 (red) and subsequently immunolabelled for VWFpp (blue) and EGFP-CD63 (anti-GFP antibody, green). TRITC-anti-CD63 can be seen in bright micro-domains on WPBs that co-localised with EGFP-CD63 micro-domains. Scale bars 2µm.

Figure 7

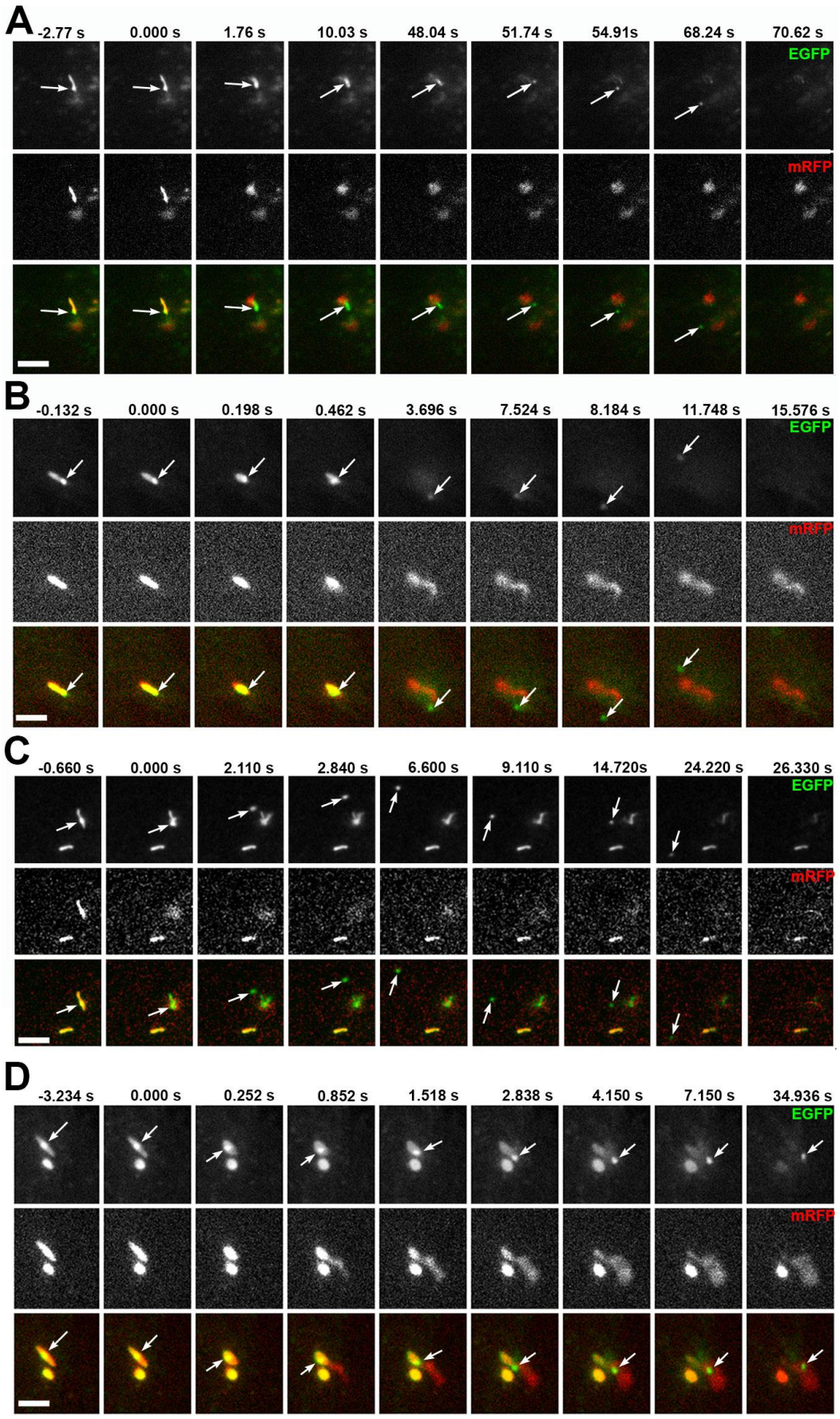
A
-2.77 s
0.000 s
1.76 s
10.03 s
48.04 s
51.74 s
54.91s
68.24 s
70.62 s
EGFP
mRFP
B
-0.132 s
0.000 s
0.198 s
0.462 s
3.696 s
7.524 s
8.184 s
11.748 s
15.576 s
EGFP
mRFP
C
-0.660 s
0.000 s
2.110 s
2.840 s
6.600 s
9.110 s
14.720s
24.220 s
26.330 s
EGFP
mRFP
D
-3.234 s
0.000 s
0.252 s
0.852 s
1.518 s
2.838 s
4.150 s
7.150 s
34.936 s
EGFP
mRFP

Figure. 7. WPB EGFP-CD63 micro-domains are secreted as discrete particles during exocytosis. A-D show examples of image montages taken from dual colour live cell videos (Supplementary videos S8, S9, S10 and S11 respectively) of EGFP-CD63 (top panels, green in colour merge) and VWFpp-mRFP (middle panels) containing WPBs prior to (frame 1) and during (frames 2-9) exocytosis evoked by histamine stimulation (100µM). Scale bars are 2µm. In each case the WPB indicated by the arrow undergoes a morphological transition from rod to spheroid shape accompanied by expulsion of VWFpp-EGFP and release of the EGFP-CD63 ILV as a discrete particle. In examples A-C the EGFP-CD63 particle diffuses out of the field of view, in D the particle remains trapped within the patch of secreted VWF. Images were acquired sequentially on a wide field microscope equipped with an Olympus UPLSAPO 100x 1.4NA objective, OptoLED epifluorescence excitation system and Andor Ixon3 EMCCD camera operating at 30 frames per second.